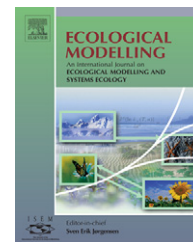


available at www.sciencedirect.comjournal homepage: www.elsevier.com/locate/ecolmodel

Plant acclimation to elevated CO₂—From simple regularities to biogeographic chaos

Vincent P. Gutschick*

Department of Biology, New Mexico State University, Las Cruces, NM 88003, USA

ARTICLE INFO

Article history:

Received 31 July 2005

Received in revised form

19 July 2006

Accepted 24 August 2006

Published on line 6 October 2006

Keywords:

CO₂

Acclimation

Models

Biogeography

ABSTRACT

Upon exposure to altered levels of CO₂, plants express a variety of acclimations to CO₂ directly, over and above acclimations to indirect changes in temperature and water regimes. These acclimations commonly include increased photosynthetic CO₂ assimilation and increased water-use efficiency with reduced N content and reduced stomatal conductance. The robust generic acclimations are explicable by combining simple models of carboxylation, stomatal control, energy balance, and functional balance. Species- or genotype-specific acclimations are overlaid on these generic acclimations. Several such specific acclimations that are often seen are readily incorporated in an extended model. These specific acclimations generate a great spread of values in key performance measures of photosynthesis, water- and N-use efficiencies, and rates of water and N use, even among C₃ species that are the focus of this work. These performance measures contribute strongly to relative fitness and thus to evolving biogeographic distributions. The spread in fitness values is so large as to impend “chaotic” shifts in biogeography (and, ultimately, evolution) that are not understandable with models specific to species or functional groups; rather, a systematic study of key physiological and developmental parameters is merited. Also merited is a coherent extension of the model used here, or similar models, to include other phenomena, including mycorrhizal associations, transience in resource availability, etc. The composition of useful approximate fitness functions from physiological and allocational responses is a major challenge, with some leads originating from the model. In the search to extract patterns of responses, arguments based on the responses being close to optimal or adaptive will be misleading, in view of the absence of selection pressure to perform adaptively at high CO₂ for over 20 million years. I offer suggestions for more useful research designs.

© 2006 Elsevier B.V. All rights reserved.

1. Introduction

Elevated CO₂ is arguably the anthropogenic change of the greatest integrated effect on the biosphere to be expected in this century, given: (1) its direct effect on photosynthesis and internal acclimations of plants, such as N content. By acclimation, I denote changes of function within a plant's life cycle, excluding immediate biochemical responses such as photosynthetic response to changing light levels, and genetic

changes between generations; (2) elevated CO₂ as a major factor in climatic change – temperature, precipitation, and general atmospheric and oceanic circulation – and (3) its complete global extent. Rising CO₂ may be implicated (Polley et al., 2003) in some vegetation changes to date such as replacement of C₄ grasses by C₃ shrubs (Buffington and Herbel, 1965). In many experiments in chambers and in free-air CO₂ enrichment (FACE) facilities – so numerous as to be cited only selectively herein – many physiological and developmental changes are

* Tel.: +1 505 646 5661; fax: +1 505 646 5665.

E-mail address: vince@nmsu.edu.

0304-3800/\$ – see front matter © 2006 Elsevier B.V. All rights reserved.

doi:10.1016/j.ecolmodel.2006.08.013

observed in plants, and inferences have been drawn for future crop and wildland productivity, biogeochemical cycling, water resources, reduction in the general competitive status of C_4 plants relative to C_3 plants, etc. Among the common changes in C_3 plants are reduced nitrogen content, reduced stomatal conductance, increased photosynthetic rate, and increased water-use efficiency (e.g., Nowak et al., 2004a). Urban (2003) has provided a comprehensive review of changes on the physiological time scale. All these changes are likely to affect plant fitness, thus, population dynamics and viability and many ecosystem functions (Körner, 2003) and subsequent evolution (Ward and Kelly, 2004). The relative value of changes in photosynthesis versus changes in N demand or in water-use efficiency, etc., varies by environment and ecosystem, giving a wide spectrum of changes in competitive status. It is therefore important to get a broad overview of the origins and consequences of these changes.

The direct responses to CO_2 form the focus of this article. The indirect effects of CO_2 's action as a greenhouse gas – changes in temperature and precipitation (T and P) regimes – are likely to become more important, but these have already received considerable attention. The direct CO_2 responses that are commonly observed can be argued, as I do here in a simple quantitative model, to arise predominantly from three physiological bases—the enzyme kinetics of carboxylation, functional balance between N uptake and N-use efficacy (photosynthetic rate per unit N) in photosynthesis (Gutschick and Kay, 1995; BassiriRad et al., 2001), and regularities in stomatal control that are captured reasonably well by the simple Ball–Berry model (Ball et al., 1987). However, overlaid on these regularities are species-specific changes (Urban, 2003; Körner, 2003). Examples include changes in root uptake capacities for N (BassiriRad et al., 2001), in relative up- and down-regulation of Rubisco content versus photosynthetic electron-transport capacity (Huxman and Smith, 2001), in phenology (Navas et al., 1997; Reekie and Bazzaz, 1991; Rusterholz and Erhardt, 1998), in tolerance of extremes of temperature (either better—Hamerlynck et al., 2000, or worse—Lutze et al., 1998), etc.

The species-specific changes show few notable regularities by family or functional group; one can cite the general lesser down-regulation of photosynthetic capacity in woody species versus nonwoody species (Nowak et al., 2004a; achieved by consistent partitioning of N to photosynthetic enzymes). This diversity should not come as a surprise. While plants broadly share adaptive responses – physiological, developmental, ecological, and evolutionary – to recurrent environmental changes such as drought and freezing, they have not experienced high CO_2 for over 20 million years (Pearson and Palmer, 2000; Long et al., 2004; critique: Boucot and Gray, 2001). Adaptive responses have not been retained in the absence of selection pressure and in the presence of both genetic drift and selection pressures for other environmental shifts. What few response complexes in any chosen species appear to be adaptive to high CO_2 are likely to result from either (1) extension in the opposite direction of responses to low CO_2 during ice ages or (2) correlation of current environmental variations with those accompanying high CO_2 —e.g., changes in precipitation amount and distribution or in temperature.

In brief, any resemblance to adaptive responses is likely to be accidental . . . and highly disparate among species, even among closely related species, as will be elaborated in Section 4.1. Species whose biogeographic ranges currently overlap strongly and which appear to participate in community assembly are likely to shift their ranges in very different patterns. Community compositions should change, in ways that expand the changes anticipated when one considers only climatic effects and not the direct effects of CO_2 . I offer the term “biogeographic chaos,” as a way of emphasizing that one may expect widespread violation of current rules elaborated for biogeographic distributions on the basis of mean climatic variables and some extremes therein. The net expectation may be projected to include global-average increases in productivity and carbon sequestration, and perhaps increased hydrologic activity (reduced evapotranspiration with rich patterns of changes in precipitation inputs). The current study focuses on changes in biogeography attendant on diversity in plant responses to CO_2 . It complements the study by Körner (2003) that predicates changes in ecosystem CO_2 response because of existing biodiversity.

In this article, I propose a simple modelling framework, focused on C_3 plants. The significant dichotomy between C_3 and C_4 responses to CO_2 has been addressed in some detail elsewhere, in their autecology and community ecology (e.g., Owensby et al., 1999; Wand et al., 1999; Poorter and Navas, 2003) as well as in biotic relations, as with herbivores (Ehleringer et al., 2002; Goverde et al., 2002). It is now expected to be accounted in analyses of experiments or predictions of global change. The changes within the domain of C_3 plants are highly significant and comprise our main focus here.

2. Methods: a simple model of regularities in autecological plant responses, emphasizing C_3 plants

The four generally observed responses to explain are as noted in Section 1: (1) an increase in photosynthetic rate per leaf area, A , less than proportional to the increase in ambient CO_2 partial pressure, C_a ; (2) a decrease in stomatal conductance, g_s ; (3) a decrease in fractional N content in tissue, f_N ; (4) an increase in water-use efficiency, WUE , or W as a compact symbol.

When combined, a few robust physiological relations predict such changes, on the time scale of the acclimated individual plant.

2.1. The enzyme and transport kinetics of photosynthesis

Model (1) is the Farquhar–von Caemmerer–Berry biochemical model of photosynthesis (Farquhar et al., 1980) for C_3 plants. (Note that a C_4 model is also well-verified: Collatz et al., 1992.) I focus here on the light-saturated regime where most photosynthesis occurs for dominant (overstorey) vegetation (e.g., Caldwell et al., 1986, for native Mediterranean vegetation, Beyschlag et al., 1990, for oats and wild oats; but compare Day and Chalabi, 1988, for cloudy climes). This rate takes the

simple form

$$A = V_{c,max} \frac{(C_c - \Gamma)}{(C_c + K_{co})} - R_d \quad (1)$$

Here, $V_{c,max}$ is the maximal carboxylation capacity, tightly related to leaf Rubisco content and thus to N content (Field and Mooney, 1986; Sinclair and Horie, 1989); C_c is the partial pressure of CO_2 in the leaf interior (at the active sites in the chloroplast); Γ is the CO_2 compensation partial pressure; and K_{co} is the effective Michaelis constant for CO_2 binding to Rubisco in the presence of O_2 . The latter two physiological parameters are functions only of temperature (and invariant O_2 partial pressure) and have limited genetic variability (see Zhu et al., 1998). R_d is the “dark” respiration, often found to be a constant fraction of net photosynthesis, A_{net} , at the temperature to which the leaves are acclimated (cf. Atkin et al., 2000; Niinemets et al., 1999).

A complementary formulation of the photosynthetic rate in terms of transport kinetics is

$$A = g'_{bsm} \frac{(C_a - C_c)}{P} \quad \text{where} \quad g'_{bsm} = \frac{1}{1/g'_b + 1/g'_s + 1/g'_m} \quad (2)$$

where P is total air pressure and g'_{bsm} is the net conductance from external air to the chloroplast sites, composed as noted from conductances in the boundary layer (g'_b), stomata (g'_s), and mesophyll liquid and wall (g'_m); the primes, as commonly used, distinguish conductances (*sans primes*) for CO_2 from conductances for water vapor.

The biochemical + transport model defines responses to the environment, when it is supplemented by environmental and physiological information. Required environmental information consists in: (1) leaf temperature, T_L , for determination of the kinetic parameters Γ and K_{co} , as well as the thermal activation of $V_{c,max}$ and R_d ; this necessitates an energy-balance model, presented in Section 2.3 below; (2) g'_b itself, which is specified directly here and is a function of windspeed and leaf shape; and (3) external air conditions: CO_2 content, C_a , to which carboxylation is tied; humidity, in any form such as relative humidity, to which stomata respond; and total air pressure, P . Required physiological information is: (1) stomatal conductance, g_s , which is responsive to environmental factors and to A itself (Ball et al., 1987; Leuning, 1995; Dewar, 1995; others); this, in turn, requires a model of stomatal response, posed in Section 2.2 following; (2) mesophyll conductance, g'_m , a function of leaf structure, taken as constant in the studies here; and (3) maximal carboxylation capacity, $V_{c,max}$; this is taken as a given under reference conditions, while its acclimatory response to changes in CO_2 and temperature requires the final (sub)model, that of functional balance in Section 2.4 below.

2.2. Stomatal control and its relation to photosynthetic capacity and water-use efficiency

Model (2) is the Ball–Berry model of stomatal conductance (Ball et al., 1987):

$$g_s = m \frac{Ah_s}{C_s} + b \quad (3)$$

Here, m and b are empirical constants, with m (dimensionless) very commonly near 10 (Ball et al., 1987; Leuning, 1990; Collatz et al., 1991; Schultz and Lebon, 1995) and b ($mol\ m^{-2}\ s^{-1}$) commonly quite small; A is assimilation, as in Eq. (1), in $mol\ m^{-2}\ s^{-1}$ (or more convenient micromolar units); and h_s and C_s are, respectively, the relative humidity and the CO_2 mixing ratio (mole fraction) at the leaf surface, beneath the leaf boundary layer. When the boundary layer has a small resistance for gas transport relative to the stomata, we may closely approximate h_s as ambient-air relative humidity and C_s as ambient-air mole fraction, C_a/P , with P the total air pressure. The Ball–Berry equation has been criticized for its empiricism and alternative models, embodying somewhat more mechanistic trends, have been proposed (e.g., Leuning, 1995; Dewar, 1995, 2002; Tuzet et al., 2003), but the Ball–Berry model often proves the best simple empirical fit (Gutschick and Simonneau, 2002 and discussion therein).

The Ball–Berry model by itself predicts several empirically verified trends, as do all related models. The coupling to A results in a near-constancy of the ratio of internal to external CO_2 partial pressures, at a stable relative humidity (beginning with early findings of Bell, 1982). The inverse dependence upon C_s reflects the common observation of reduced g_s at high CO_2 . Given the gain in A at high CO_2 , however, one might expect relatively small changes in g_s with changes in CO_2 (as C_a). The significant reductions in g_s often observed at high CO_2 are seen to be more the result of acclimation in photosynthetic capacity, $V_{c,max}$, which can be attributed in large measure to functional balance responses (part 2.4). The coupling of g_s to humidity results in decreased g_s and presumably adaptive increase in water-use efficiency, WUE, at low humidity. Similarly, increased leaf temperature at constant water vapor content of air (as partial pressure) reduces h_s and g_s . In both g_s trends, there is a positive feedback, given that low h_s leads to low g_s and low A , further reducing g_s . The Ball–Berry model can exhibit excessive feedback in some conditions. More complete models (e.g., Tuzet et al., 2003) are more accurate but are far more challenging to parametrize; the Ball–Berry model serves as a good starting point and has very stable parameter values among many species (Gutschick and Simonneau, 2002). A further development of useful approximations to trends in A , g_s , and WUE is given in Appendix A.

There is evidence that stomatal sensitivity, particularly to humidity, changes when ambient CO_2 levels change (e.g., Bunce, 1998). Consequently, the model allows for the Ball–Berry slope, m , to have a power-law dependence upon internal CO_2 , C_i , to which quantity g_s seems to respond (Mott, 1988):

$$m = m_0 \left(\frac{C_i^0}{C_i} \right)^c \quad (4)$$

One might also include more detailed acclimation of the humidity (h_s) response to changes in CO_2 (Bunce, 1998).

2.3. Energy balance for the determination of leaf temperature

Changes in stomatal conductance alter the leaf transpiration rate, altering, in turn, the leaf temperature, T_L , and the

kinetic constants dependent upon temperature. The change in steady-state energy balance is of most interest. The net energy storage rate is written in terms of five energy flux densities (Q_i) at the leaf surface (Model (3)) as:

$$S = 0 = Q_{SW}^+ + Q_{TIR}^+ - Q_{TIR}^-(T_L) - Q_E(T_L) - Q_C(T_L) \quad (5)$$

The terms refer, respectively, to shortwave radiant gain, thermal infrared radiant gain, thermal infrared radiant loss, latent heat loss from transpiration, and convective heat loss. The last three terms only depend upon T_L , as indicated.

Many environmental conditions and leaf parameters are involved but they may be inferred to a reasonable accuracy, particularly given that only shifts in T_L are relevant. The TIR gain and the TIR loss may be written, respectively, as

$$Q_{TIR}^+ = \varepsilon\sigma(T_{sky}^4 + T_{terr}^4); \quad Q_{TIR}^- = 2\varepsilon\sigma T_{L,abs}^4 \quad (6)$$

Here, ε is the TIR absorptivity (and emissivity) of the leaf and σ is the Stefan-Boltzmann constant. Three absolute or Kelvin temperatures appear. $T_{L,abs}$ is the absolute leaf T . T_{sky} is the effective radiative temperature of the sky (taken as $T_L - 20^\circ\text{C}$ as a common condition in nonhumid locations); T_{terr} is the effective radiative temperature of the terrestrial surroundings (taken as T_L). Given the closeness of ε to unity (about 0.96) and the insensitivity of calculated T_L shifts to this parameter, we henceforth replace it with unity.

The transpirational cooling is

$$Q_E^- = \lambda g_{bs} \frac{e_i(T_L) - e_a}{p} \quad (7)$$

Here, λ is the heat of vaporization of water, g_{bs} is the conductance through the boundary layer plus stomata ($=1/[1/g_b + 1/g_s]$), and the two partial pressures of water vapor (WVP) are, respectively, for external air (e_a) and the leaf interior (e_i). From fixed parameters and the stomatal control model, one knows g_{bs} and P , and e_i is almost exactly the saturated vapor pressure at leaf temperature. The value of e_a is inferred from the value of h_s that one sets at reference conditions. Given that h_s is defined as the ratio of WVP at the leaf surface beneath the boundary layer (e_s) and e_i , one may solve for e_a algebraically. One may readily verify that $e_a = e_i[h_s - (1 - h_s)g_s/g_b]$. With these substitutions, all the terms in Q_E^- are set.

The convective loss is formulated as the standard Newton's law of cooling. In terms of the molar heat capacity of air at constant pressure ($C_{P,mol}$), the boundary-layer conductance (approximated well as equal for heat and water vapor), and the leaf and air temperatures, this is

$$Q_C^- = C_{P,mol}g_b(T_L - T_a) \quad (8)$$

The final term is the shortwave radiant energy gain. One commonly expresses this in terms of leaf absorptivity and solar shortwave energy flux density, but it is not necessary to know such details. It suffices to fix Q_{SW}^+ as the residual in Eq. (5); it will be constant in all the changes in CO_2 , etc. that are modelled here. The full Fortran program calculates the attendant flux density of photosynthetically active radi-

ation, to confirm that it is consistent with light saturation of photosynthesis.

Changes in any environmental or physiological parameter require solving Eq. (5) anew. Changes in T_L are modest, so that a simple Newton-Raphson iterative search for the new root of the equation always suffices. As the new T_L is obtained, the model updates the thermal activation functions for $V_{c,max}$, Γ , and K_{co} in the photosynthesis model, using parameters derived by de Pury and Farquhar (1997). The model assumes that there is no significant change in dark respiration as a fraction of net photosynthesis, following the results of Atkin et al. (2000) and Niinemets et al. (1999).

2.4. Functional balance in nitrogen uptake and use, and the necessity of lower N content

Model (4): the functional balance model of plant N uptake and N use in photosynthesis (Gutschick and Kay, 1995; BassiriRad et al., 2001). Nitrogen is the focus in this model, as being the nutrient most commonly limiting plant performance; other nutrients, especially phosphorus, are also limiting over large areas and, moreover, limiting plant responses to CO_2 (Urban, 2003). Some modification of the model being presented here is necessary to consider phosphorus (*ibid.*). Full derivations with experimental tests are given in the two references cited. In brief, this model predicts N content, f_N , and relative growth rate, RGR, from a knowledge of root N-uptake rate per mass, v , photosynthetic N-use efficacy as photosynthetic rate per mass of N, p^* , two mass allocation parameters (root:shoot ratio, r , and fraction of shoot mass as leaf mass, α_L), and the biosynthetic efficiency of converting raw photosynthate into biomass, β . The predictions are that RGR rises as the square root of p^* and that f_N falls as the inverse factor. Higher CO_2 increases p^* , and leads to (other factors nearly equal) a fall in f_N that is of the common magnitude and that is seen as not only adaptive but mandated by growth balances.

One equates the relative growth rate limited by photosynthesis, $R_{P,L}$, with the relative growth rate limited by N uptake, $R_{N,L}$. These cannot get significantly out of balance over a number of doublings in plants size; if the plant C content underwent six doublings while the N content underwent five doublings (only a 17% mismatch in the rates), the C:N ratio would double, which is not a common occurrence in vegetative growth. The N-limited rate is readily derived. Consider a plant of total dry mass m , with a root mass m_r , an uptake rate v , and a fractional N content f_N (both v and f_N assumed substantially stable over the time frame of interest). The rate of dry mass gain, multiplied by f_N , is clearly the N uptake rate of the whole plant:

$$f_N \frac{dm}{dt} = m_r v \quad (9)$$

The relative growth rate is defined as $(1/m)(dm/dt)$, so, writing m_s for the shoot dry mass and using the definition of root:shoot ratio as m_r/m_s , we obtain

$$R_{N,L} = \frac{1}{(m_r + m_s)} \frac{m_r v}{f_N} = \frac{r}{(1+r)} \frac{v}{f_N} \quad (10)$$

The photosynthesis-limited rate is slightly more complex to derive. It equals the whole-plant photosynthetic rate, A_p ,

multiplied by the biosynthetic efficiency, β . The whole-plant rate equals the rate per leaf area, A , multiplied by the leaf area, a_p :

$$\frac{dm}{dt} = \beta A_p = \beta A a_p \tag{11}$$

The leaf photosynthetic rate responds to its N content per area, N_a , in near proportion (Field and Mooney, 1986; Sinclair and Horie, 1989); in turn, we may express N_a as fractional N content (of leaves, $f_{N,L}$) multiplied by dry mass per unit leaf area, $m_{L,a}$:

$$A = p^* N_a = p^* f_{N,L} m_{L,a} \tag{12}$$

This introduces the photosynthetic N-use efficacy, p^* , measured in mol (or μmol) $\text{m}^{-2} \text{s}^{-1}$ per g_N . This will change in close proportion to the CO_2 partial pressure in the leaf, C_i ; p^* equals A/N_a and thus, by Eq. (1), it equals $(V_{c,\text{max}}/N_a)(C_i - \Gamma)/(C_i + K_{co})$. The magnitude of $V_{c,\text{max}}$ is closely tied to Rubisco content and thus to N content, so that the factor $(V_{c,\text{max}}/N_a)$; call it G , for use in later modelling) varies little, in most cases, even as a plant acclimates to CO_2 changes. Now we need express the whole-plant leaf area as the leaf mass, m_L , divided by mass per leaf area, and express m_L as the allocation fraction α_L multiplied by shoot mass:

$$a_p = \frac{m_L}{m_{L,a}} = \frac{\alpha_L m_s}{m_{L,a}} \tag{13}$$

Now we combine the factors to obtain

$$\frac{dm}{dt} = \frac{\beta p^* f_{N,L} m_{L,a} \alpha_L m_s}{m_{L,a}} \tag{14}$$

The factors of $m_{L,a}$ cancel. We can then rewrite the relative growth rate, using $m = m_r + m_s$ again, as

$$\frac{1}{m} \frac{dm}{dt} = \frac{1}{m_s + m_r} \frac{\beta p^* f_{N,L} \alpha_L m_s}{m_s + m_r} = \frac{\beta p^* \alpha_L}{1+r} f_{N,L} \tag{15}$$

Now we equate the two relative growth rates, obtaining an equation for N content. We take the leaf N content as a factor q (>1) multiplied by whole-plant N content, and we obtain

$$\frac{r}{(1+r)} \frac{v}{f_N} = \frac{\beta p^* \alpha_L q}{(1+r)} f_N \tag{16}$$

Rearranging, we get

$$f_N^2 = \frac{rv}{\beta p^* \alpha_L q} \Rightarrow f_N = \sqrt{\frac{rv}{\beta p^* \alpha_L q}} \tag{17}$$

This form shows all the common qualitative behavior— f_N increases with N uptake rate (but only as the square root), and it decreases as p^* increases (less N suffices; again, the behavior is as the square root) and as allocation to leaves increases. For a doubling of CO_2 and, hence, a near-doubling of p^* , one expects f_N to decrease by a factor of $1/\sqrt{2}$, that is, to drop by about 29%. Additional discussion is given by BassiriRad et al. (2001).

We can complete the functional balance model by substituting this expression f or N content into either expression for

relative growth rate, R , obtaining

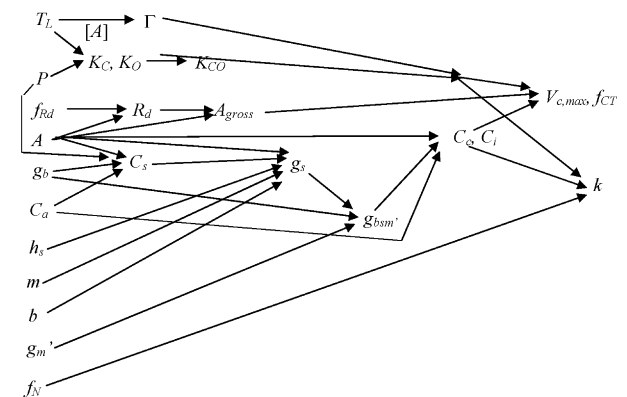
$$R = \frac{\sqrt{rv\beta p^* \alpha_L q}}{1+r} \tag{18}$$

This, too, captures common behavior. For one, relative growth rate increases as N uptake increases or as p^* increases, but only as the square root.

2.5. Mathematical solutions, and additional features

How do all these phenomena or behaviors combine? We must solve all these equations simultaneously. A detailed schema is given in Table 1, which indicates all the physiological and environmental operating points, and Fig. 1, which shows the sequence of computations. First, we must determine the basic environmental and physiological parameters in the reference conditions of normal CO_2 . We specify the initial values of the environmental variables C_a , P , h_s , g_b , and T_L , and the physiological variables m , b , A_{net} , g'_m , f_N , and R_d . These comprise a complete description, from which we compute: (1) several more fundamental physiological descriptors, particularly the carboxylation capacity, $V_{c,\text{max}}$, and a combination of parameters $(rv/[\beta\alpha_L q])$ that we approximate as invariant in the functional-balance model; (2) initial measures of performance, over and above the already-specified values of A and f_N . Specifically, we compute initial values of stomatal conductance (g_s^0) internal and chloroplastic CO_2 partial pressures (C_i^0 and C_c^0) transpiration rate (E^0), water-use efficiency ($\text{WUE}^0 = A^0/E^0$),

For photosynthesis function:



For energy balance of leaves:

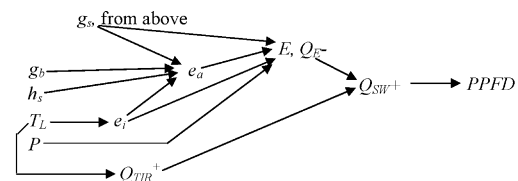


Fig. 1 – Chain of computations for deriving all the operating points of a plant from knowledge of a basis set of operating points (those occurring at the left edge). See Table 1 for specification of the process equations used in each computation. Calculations for photosynthesis are denoted at the top of the figure; calculations for energy balance and leaf temperature are denoted at the bottom.

Table 1 – Schema for computing operating point of plant and the changes induced by changes in atmospheric CO₂

Initial physiological and environmental quantities, in order of appearance in Fig. 1

- T_L = Leaf temperature
- P = Ambient air pressure
- f_{Rd} = Fraction of gross photosynthesis as dark respiration
- A = Net CO₂ assimilation rate per unit leaf area
- g_b = Boundary-layer conductance of leaf to CO₂, per unit leaf area
- C_a = Ambient CO₂ partial pressure
- h_s = Relative humidity at leaf surface, beneath boundary layer
- m = Slope of Ball–Berry relation for stomatal conductance
- b = Intercept of Ball–Berry relation
- g'_m = Mesophyll resistance to CO₂ transport
- f_N = Fractional N content in tissue

Derived quantities for photosynthesis

- Γ = CO₂ compensation partial pressure for photosynthesis (from published temperature dependence; cf. Zhu et al., 1998)
- K_c, K_o = Binding constants for CO₂, O₂ to Rubisco enzyme (*ibid.*)
- $K_{co} = K_c(1 + O/K_o)$ = Effective Michaelis constant for CO₂ binding to Rubisco in the presence of O₂ (O = partial pressure of O₂)
- R_d = Dark respiration rate per leaf area, as $f_{Rd}A_{gross}$
- A_{gross} = Gross assimilation rate per leaf area = $A + R_d = A/(1 - f_{Rd})$
- C_s = CO₂ mixing ratio (mol mol⁻¹) at leaf surface, beneath boundary layer = $C_a - AP/g'_b$, from a transport law; g'_b = boundary layer conductance for CO₂ = $0.72g_b$
- g_s = Stomatal conductance for water vapor, per leaf area, from Ball–Berry relation, Eq. (3)
- g'_{bsm} = Total physical conductance for CO₂ per leaf area, from Eq. (2), right-hand side
- C_c, C_i = Partial pressure of CO₂ at chloroplasts or in leaf interior air spaces, from Eq. (2), left-hand side
- f_{CT} = Fractional saturation of Rubisco in CO₂ = $\sqrt{(C_c - \Gamma)/(C_c + K_{co})}$; used in computing photosynthetic N-use efficacy
- $V_{c,max}$ = Maximal carboxylation (CO₂-fixation) rate of Rubisco, per leaf area, obtained by inverting Eq. (1)
- $k = f_N f_{CT}$ = Constant in adjustment of tissue N content upon changes of C_a and upon acclimation

Initial information for energy balance

- g_s , the stomatal conductance, is taken as derived above; g_b, h_s, T_L , and P are repeated as known quantities

Derived quantities for energy balance

- e_i = Partial pressure of water vapor in leaf interior, computed from standard formulas
- e_a = Partial pressure of water vapor in ambient air; equate expressions for transpiration rate across boundary layer and across stomata, $E = g_b(e_s - e_a)/P = g_s(e_i - e_s)$, and solve for e_a
- Q_{TIR}^+ = Total energy flux density of thermal infrared radiation incident per leaf area (both sides), from Eq. (6)
- E = Transpiration rate per leaf area
- $Q_E^- = \lambda E$ = Rate of latent heat loss per leaf area, from Eq. (7)
- Q_{SW}^+ = Rate of shortwave solar radiation gain per leaf area; solve Eq. (5), assuming $Q_C^- = 0$ in original operating point, i.e., that T_L = air temperature
- PPFD = Photosynthetic photon flux density =
(fraction of shortwave energy in PAR) $\times Q_{SW}^+$ / (energy per mole of photons)

Note that there is no need for explicit computation of factors in the functional balance relation (Eq. (17)); only changes in partitioning need be computed, below)

Quantities used to describe changes in plant function at elevated CO₂

- New C_a
- U = Multiplicative factor for scaling N uptake rate
- P_L = Multiplicative factor for scaling the allocation of whole-plant biomass to leaves
- P_R = Multiply factor for scaling partitioning of N to Rubisco in leaves
- q = Exponent in rescaling Ball–Berry slope, m , according to change in C_i (Eq. (4))

Derived quantities for changes in plant function

- $f_{acclim} = \sqrt{U/(P_L \times P_R)}$ = Factor in rescaling of maximal carboxylation capacity, $V_{c,max}$

Outline of method of calculating changes in plant function (commented Fortran program gives complete details)

- Specify new C_a and factors U, P_L, P_R ; compute f_{acclim}
- Guess new values of T_L and C_c ; use old g_s as initial estimate of stomatal conductance; set bounds for estimating C_c (these can be recomputed if the search fails in stated bounds)
- Perform a binary search for C_c
 - From current T_L , compute Γ, K_{co}
 - From current C_c , fixed f_{Rd} , and the above, compute A from Eq. (1)
 - Solve for value of h_s that is consistent with transpiration rate and Ball–Berry relation (Eq. (3)):
 - $g_s = mA_h_s/C_s + b$ —denote as $kh_s + b$
 - e_s = Partial pressure of water vapor at leaf surface, beneath boundary layer = $e_i - EP/g_s = e_i - g_b(e_s - e_a)/g_s$
 - Divide by e_i and use $h_s = e_s/e_i$; obtain quadratic equation in h_s ; solve for h_s

Table 1 (Continued)

Now having A and h_s , solve Ball–Berry equation for new value of g_s
 Compose function representing error in consistency between transport relation for photosynthesis (Eq. (2)) and the enzyme-kinetic and Ball–Berry equations used to estimate A and g_s
 $F = A - g'_{\text{bsm}}(C_a - C_c)/P$ (see Eq. (2), left-hand side)
 Using new estimate of g_s , update the estimate of T_L : revise the estimate of latent heat loss rate, Q_c^- ; solve nonlinear Eq. (5) for T_L , by iterative Newton–Raphson method
 Using new estimate of C_i , update the estimate of Ball–Berry slope, m (Eq. (4))
 Subdivide the search interval in C_c to find the region where F changes sign (must contain value of C_c that makes $F=0$, the completely consistent solution of all equations)
 Iterate this search for predetermined number of times, n , reducing uncertainty in C_c to fraction $1/2^n$ of original search range

and photosynthetic N-use efficacy, $(\text{PNUE}^0 = A^0/f_N^0)$; (3) several basic environmental parameters in the energy-balance equation, as noted in Section 2.3.

Having the descriptors of the reference case in hand, we now consider performance when external CO_2 , C_a , changes. Even without physiological acclimation, such as in N content and carboxylation capacity, many variables change, as determined by the combined four models. There is no “closed-form” solution to the combined models, that is, no simple algebraic expression for the final values of A , f_N , g_s , or C_i in terms of the environmental and physiological/allocational parameters. We must solve the equations numerically. Two nested iteration loops suffice. In the outer loop, one iterates for the value of $V_{c,\text{max}}$ that is consistent with the photosynthetic and functional-balance models. The inner loop implements a binary search for the value of chloroplastic CO_2 , C_c that is consistent with the photosynthetic rate as Eq. (1) and as Eq. (2), as well as with the stomatal model, Eq. (3). In brief, one computes an error function, F , as the difference of A expressed in these two equations, and using a value of g_s computed as $mAh_s/C_s + b$ in the transport equation, Eq. (2). A Fortran program, quite compact and fully commented, has been generated and posted on my website (<http://biology-web.nmsu.edu/vince>).

Several physiological acclimations are quite prominent in plants and are also important in CO_2 responses; they add very little computational complexity. These changes, which are quite species-specific, include changes in the allocational parameters r , α_L , and G , in the N-uptake rate, and in the Ball–Berry slope, m . There are reports of shifts in r ; while some were artifacts of experimental conditions (Stulen and Den Hertog, 1993; Long et al., 2004), the origins of such shifts display some complexity (*ibid.*; Friedlingstein et al., 1999; Pritchard et al., 1999), particularly a dependence on N and water limitations (van Noordwijk et al., 1998). Nitrogen uptake rates also change, some very negatively and some very positively, and some relatively little (Fig. 2, from BassiriRad et al., 2001). In the compete model, I therefore allow a rescaling of the product, rv (Eqs. (17) and (18)), by a factor U (for “Uptake”). Leaf allocation shifts modestly in some species (e.g., Poorter and Nagel, 2000; Urban, 2003). The complete model incorporates a factor P_L (“Partitioning to Leaves”) that multiplies the original allocation fraction, α_L . Fractional allocation of N to Rubisco can also shift, changing the proportionality of $V_{c,\text{max}}$ to N per leaf area. This has been implicated in lesser down-regulation of $V_{c,\text{max}}$ in woody species as a group (Nowak et al., 2004a). Changes in allocation have also been traced directly to

altered amounts of enzymes for utilizing photosynthate (van Oosten and Besford, 1995). In the complete model, I allow a rescaling of this proportionality by a factor P_R (“Partitioning of Rubisco”). The extra growth of the plant itself at higher C_a may deplete soil N and reduce v ; a full systems model will illuminate such effects, but is not pursued here. Fourth and finally as a species-specific acclimation, the Ball–Berry slope may change, as formulated approximately in Eq. (4) in Section 2.2.

3. Results of simulations

3.1. Prediction of basic changes in plant performance

Simulations were run with the four basic models (carboxylation kinetics, Ball–Berry stomatal control, energy balance, and functional balance) at three values of ambient CO_2 mixing ratio: the current value near $370 \mu\text{mol mol}^{-1}$ (commonly cited as ppmv), the pre-industrial value of $280 \mu\text{mol mol}^{-1}$, and the value of $550 \mu\text{mol mol}^{-1}$ projected for late this century and used in many FACE experiments. The simulations yielded values of five variables likely to be important in plant growth, survival, and competition: stomatal conductance (g_s); photosynthetic CO_2 assimilation (A); water-use efficiency $\text{WUE} = E/A_s$; $1/f_N$ as a measure of N demand per unit biomass growth; and photosynthetic N-use efficacy, $\text{PNUE} = A/f_N$. All the values followed the expected trends as CO_2 increased. First, g_s decreased by 28% (i.e., by a factor 0.72) as C_a rose from pre-industrial levels (PIL) to current levels (CL), and then decreased by 37% as C_a rose from CL to future levels (FL). (Fig. 3a. This estimate can be compared with observed changes, and also with changes in stomatal number density per unit leaf area, which can be even larger: Woodward and Kelly, 1995; Morison, 1998.) The four other measures all increased (Figs. 3a–d, solid line in each figure): A by 8% (a factor of 1.08) in both stages of CO_2 increase; W by 23% and then by 35%; $1/f_N$ by 19% and then by 25%; and PNUE by 29% and then by 35%. These changes are certainly very relevant to competition with C_4 species, for which the corresponding changes in A and PNUE are notably smaller than for C_3 species; their changes in WUE are significant (Ghannoum et al., 2000, 2001; Poorter and Navas, 2003; Wand et al., 1999).

What is of strong interest for competition and biogeographic shifts among C_3 plants is the variation of these gains between plants (*ibid.*) displaying common species-specific acclimations, over and above the generic acclimation embodied in the three basic models. Among the many combinations

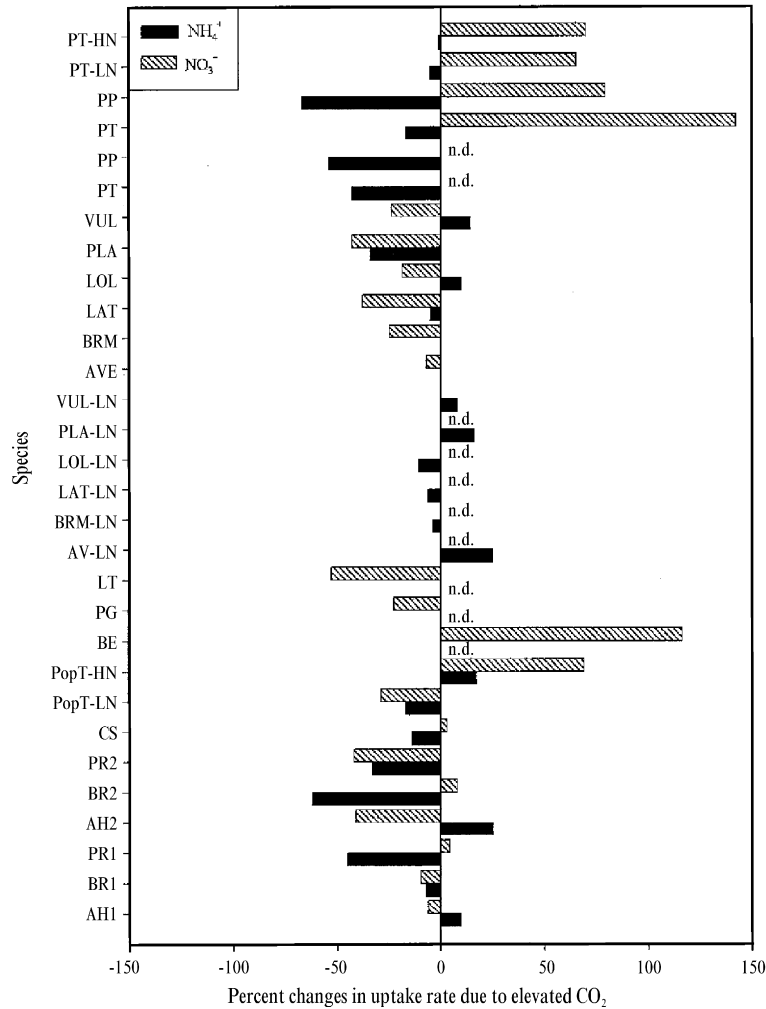


Fig. 2 – Diversity among plant species in changes in N uptake rates, upon exposure to elevated CO₂ (1.5–2× ambient). Species identities and literature references are given in BassiriRad et al. (2001, Fig. 2), from which this figure is duplicated with permission.

that likely occur, I consider four that may be more common: (1) increased N-uptake capacity with increasing CO₂. I consider a common increase of 20% as CO₂ rises from current to future levels (BassiriRad et al., 2001). Presuming that this represents a power-law dependence of N-uptake, the exponent is then estimated as 0.45, which predicts a corresponding drop of N uptake by 12% on dropping CO₂ from current to pre-industrial levels (CL to PIL); (2) decreased N-uptake capacity, by the inverse factors (to 1/1.20 = 83% on going from CL to FL, and an increase by a factor of 1/0.88 = 1.14 on going from CL to PIL); (3) reduction of the Ball–Berry slope, m , by a power-law in C_i (exponent = -0.25); (4) increased N-uptake capacity and increased partitioning of leaf N to Rubisco enzyme (by a factor of 1.2); the increased partitioning is observed in woody species as a group (Nowak et al., 2004a).

3.2. Requirement for complete set of models

The effects of acclimations vary with the completeness of the models. Fig. 4 shows predictions of the simultaneous shifts in

assimilation and water-use efficiency under changes in CO₂, for five different parametrizations. Simulations that ignore the finitude of the boundary-layer conductance (setting it to a very high value; curves labelled “Boundary layer absent”) effectively ignore energy balance and changes in T_L . Simulations with realistic values of g_b (curves labelled “Realistic boundary layer”) yield notably smaller changes in performance. The reasons are readily discerned. In both choices of boundary layer, the surface relative humidity, h_s , is stipulated as 0.5. Consequently, the water vapor pressure at the leaf surface, e_s , is the same with both choices. The ambient-air water vapor pressure, e_a , is lower than e_s by the required drop through the boundary layer, $-EP/g_b$. Thus, e_a is considerably lower in the case of the realistic boundary layer. Upon an increase in ambient CO₂, stomatal conductance, g_s , decreases in both cases. However, the decrease in h_s is pronounced in the case of the realistic boundary layer. The drop in g_s is amplified by the Ball–Berry response, so that A has only a modest increase, in contrast to the case with the boundary layer being absent. Furthermore, heat transport is retarded by the boundary layer,

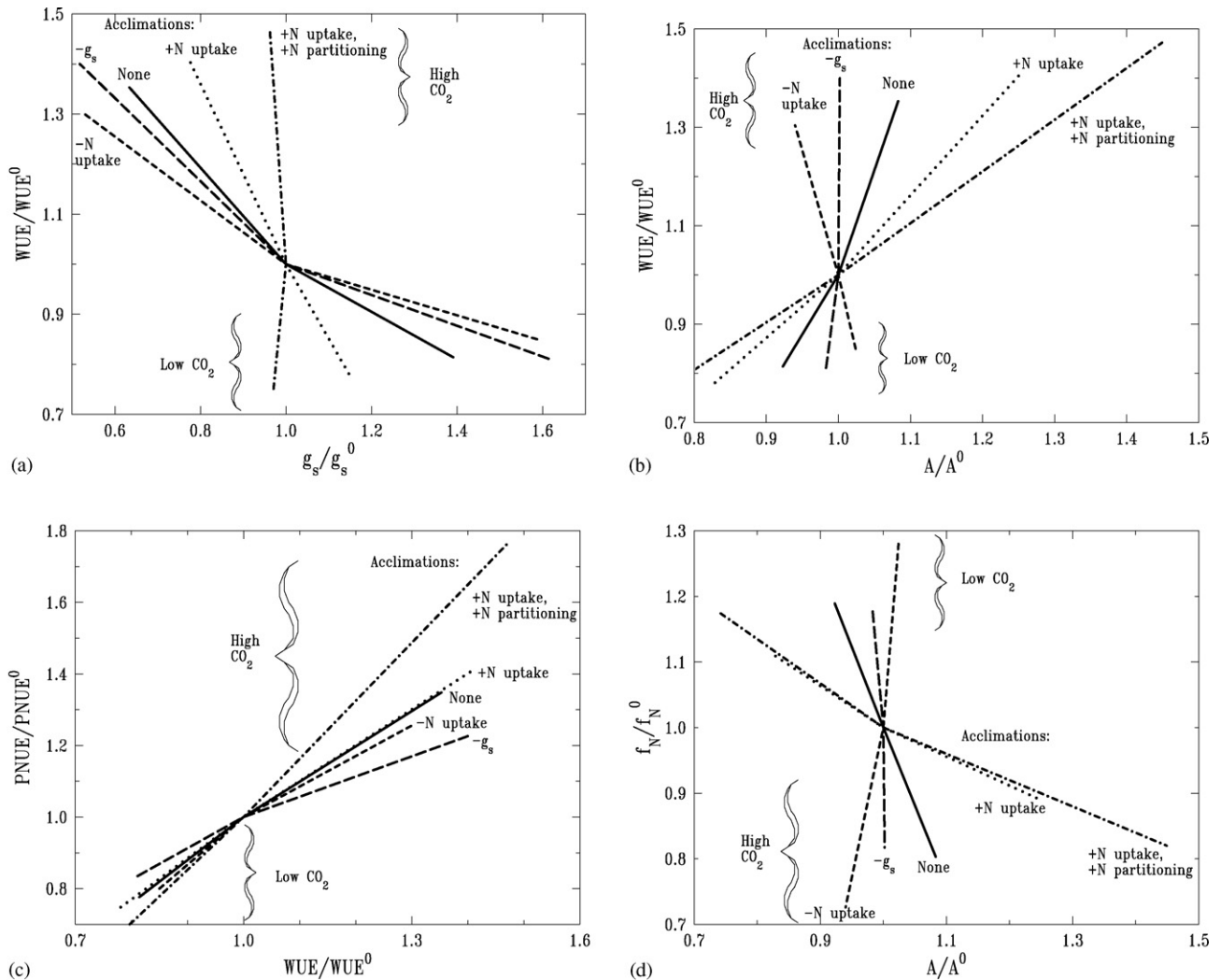


Fig. 3 – Predictions of relative changes occurring jointly in photosynthetic CO_2 assimilation, A , water-use efficiency, WUE , photosynthetic N-use efficacy, $PNUE$, tissue N content, f_N , and stomatal conductance, g_s , upon shifting from current CO_2 levels ($370 \mu\text{mol mol}^{-1}$; central point taken as 1.00 on both axes) to past levels ($280 \mu\text{mol mol}^{-1}$; labelled “Low CO_2 ”) or future levels ($550 \mu\text{mol mol}^{-1}$; labelled “High CO_2 ”). Curves represent the behavior modelled with no special acclimations (“None”) or with the four specific acclimation combinations noted in the text: (a) increased N uptake capacity with increasing CO_2 ; (b) decreased N uptake capacity; (c) reduction in Ball–Berry slope; and (d) increased N uptake combined with greater partitioning of N to Rubisco. A wide spread in combined performance measures, particularly in A and f_N , is apparent. Variations in WUE with type of acclimation are moderate.

raising leaf temperature when g_s decreases and, consequently, so does transpirational cooling. The heating effect is absent if the boundary layer is absent.

Among the three curves simulated with a realistic boundary layer, differences in the stomatal control parameters result in some significant differences, but only in assimilation, not in water-use efficiency. The curve labelled “Normal g_s ” results from using “standard” values of the Ball–Berry slope, $m=10$, and intercept, $b=0.02$. A decrease in the Ball–Berry intercept, setting b to 0.003, makes g_s more responsive to changes in humidity. Therefore, changes in g_s are amplified by the direct response of g_s to leaf-surface CO_2 mixing ratio, C_s . Again, this is an example of positive feedback. In consequence, A increases by only 4.4% at higher CO_2 ; with the “normal” value of b , the increase in A is 8.3%. The third curve, labelled “ A_{gross} ”,

alters the Ball–Berry model so that A in Eq. (3) is interpreted as gross assimilation, not net assimilation. The rationale for this change is that g_s is probably responding to an internal carbon flux (e.g., Santrucek and Sage, 1996), but it has not been tested experimentally whether this is a gross flux or a net flux (after respiratory losses of CO_2 , R_d). Even though R_d is postulated to be the same fraction of gross A in all simulations, this change in Ball–Berry response predicts a smaller increase in A (only 5.8%) at high CO_2 . The positive feedback from g_s to h_s to g_s again is accentuated, dropping g_s by a factor of 0.602 compared to a factor of 0.633 when g_s responds to net A .

A conclusion is that a realistic g_b is quite important, and that some care must also be taken with the modelling of stomatal control. Thus, only the simulations with $g_b = 1 \text{ mol m}^{-2} \text{ s}^{-1}$ and standard Ball–Berry parameters are used in subsequent

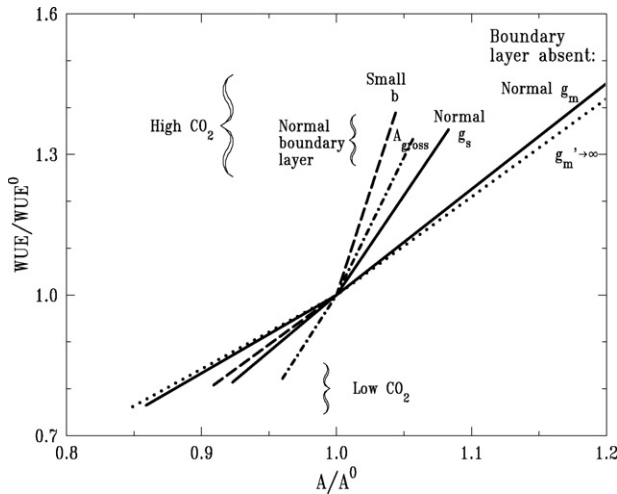


Fig. 4 – Importance of realistic submodels in predictions of plant performance. Two curves marked “Boundary layer absent” have boundary-layer conductance g_b set to $1000 \text{ mol m}^{-2} \text{ s}^{-1}$, disallowing changes in leaf energy balance and surface relative humidity; remaining curves use realistic $g_b = 1 \text{ mol m}^{-2} \text{ s}^{-1}$. Of the former curves, one uses normal magnitude of leaf mesophyll conductance (air-space and liquid-phase), $g'_m = 1 \text{ mol m}^{-2} \text{ s}^{-1}$; other uses $g'_m = 1000 \text{ mol m}^{-2} \text{ s}^{-1}$, forcing CO_2 partial pressures in leaf air space to equal that at chloroplast ($C_i = C_c$). Three curves with normal g_b represent three simulations of stomatal control: “Normal g_s ” uses Ball–Berry parameters $m = 10$, $b = 0.02 \text{ mol m}^{-2} \text{ s}^{-1}$; “Small b ” changes b to $0.003 \text{ mol m}^{-2} \text{ s}^{-1}$, enhancing feedback in g_s response to humidity and assimilation; “ A_{gross} ” replaces net assimilation (gross minus respiration, or $A_{\text{gross}} - R_d$) with gross assimilation in Ball–Berry relation, Eq. (3).

analyses in Figs. 3a–d. It should also be noted that the inclusion of dark respiration does not change results, provided that net photosynthesis in the base case remains the same and, that R_d acclimates to growth temperature as proposed, and that stomatal conductance responds to net and not gross photosynthesis. Only carboxylation capacity as $V_{c,\text{max}}$ shifts, to increase gross photosynthesis when respiration is included in the model.

3.3. Combination of performance measures are predicted to change in diverse patterns

The results in Fig. 3a–d display how shifts in g_s , A , W' , f_N , and PNUE combine among the five different cases of acclimation behavior (base case and the four cases chosen above). The relation to CO_2 levels is clearly labelled, and the center point is always the current level of $370 \mu\text{mol mol}^{-1}$, considered without any acclimations (acclimation is only to changing CO_2). It is apparent, first, that the spread of gains is significant: between 30 and 47% in WUE (that is, in W'), on going from 370 to $550 \mu\text{mol mol}^{-1}$; between -6 and $+45\%$ in A ; and between 23 and 77% in PNUE. Changes in f_N range between -17 and -11% . Changes in g_s range from -48 to -22% . Second, the combinations of gains vary even more, without strong

tradeoffs—that is, without strong correlations or constraints that might be expected, such as between g_s and WUE (Fig. 3a). Similarly, one might expect high A to occur at low WUE, in general, but Fig. 3b shows two cases that differ radically, even having opposite slopes, as a consequence of opposite acclimations in N uptake and partitioning. Significant variations in PNUE are, however, more tightly related to WUE (Fig. 3c). The wide variations in both A and f_N are strikingly uncoupled (Fig. 3d).

In addition to the wide variations in performance measures that are almost free of tradeoffs, other trends are of interest. The ratio C_i/C_a varies little at high C_a , only from 0.62 to 0.65, with one exception (0.59), despite an apparent rebalancing of g_s to photosynthetic capacity (see Eq. (A3) in Appendix A). This stability reflects that the ratio $g_s/V_{c,\text{max}}$ depends almost solely upon Ball–Berry slope (Eq. (A7) in Appendix A). It is also worth remarking that PNUE shows a slight gain even with increased N uptake rate, contrary to the expectation that resource surfeits commonly are accompanied by decreased resource-use efficiencies (more properly termed efficacies, because they are not unitless).

3.4. Challenges in relating changes in performance to changes in fitness and biogeography

One may inquire further, asking how changes in the several performance measures translate into changes in plant fitness, hence, into changed competitive status, abundance, and biogeographic distribution. No simple translation exists, for a number of reasons, including shifts of importance with life stage. For example, photosynthetic rate may be important in early growth for height gain, while WUE might be important later with incipient water shortages, and N frugality (as $1/f_N$) or PNUE might be important over long time scales as N becomes immobilized in all biomass. Even with coarser resolution, such as season-total water availability, the importance of a performance measure such as WUE varies, declining as expected at high availability (e.g., Nowak et al., 2004a, Fig. 8). Finally, fitness has a number of components beyond resource use for simple growth, such as seed number, seed weight, etc. (Ward and Strain, 1997).

While being aware of these reservations, I offer exploratory estimates of fitness changes. Consider that fitness in simple population models is commonly measured as a genotype's growth rate, r (Futuyma, 1998). Between any two populations that are relatively homogeneous internally, differences in r are in the same ratio as differences in individual-plant relative growth rate, RGR. In turn, RGR is directly proportional to photosynthetic rate, A , as indicated in Eq. (15) here. The relation changes and differentials in growth between plants diminish markedly if growth rate is curtailed by mutual leaf shading and other developmental shifts; the slow plant “catches up” if the two genotypes grow in separate patches (see Gutschick, 1987, pp. 25–27). Therefore, one may project to a first approximation that relative fitness is measured by relative performance in A , when growth rate is critical. (For a significantly more sophisticated treatment, extending also to genotype evolution, see Ward and Kelly, 2004.) Consequently, among the five acclimation scenarios, a rough estimate is that the spread in fitness as measured by r may vary by the ratio of $1.45/0.94$ (between a

gain of 44% and a 6% loss in A), which is 1.54. This 54% range in relative fitness, if realistic, is of great import; in evolution, selection differentials of several percent are considered large (Kimura, 1983). Even a 10% gain in A, compounded over a typical 10 doublings of plant mass from seed to adult, results in one additional doubling, a gain of 100%.

When water is most limiting, WUE becomes the performance measure most closely related to fitness. However, relative growth rate is not proportional to WUE, which is related to total growth. A 10% gain in WUE translates to a simple 10% gain in final mass, assuming all the water is used, as is commonly observed in intact ecosystems (Ellsworth, 1999; Körner, 2001; Nowak et al., 2004b). We may compute an effective gain in r in this case. If a plant grows exponentially, we have the simple relations among initial mass (say, of the seed), m_0 , final mass, m , growth duration, t , and relative growth rate, r :

$$m = m_0 e^{rt} \rightarrow r = \frac{1}{t} \ln \left(\frac{m}{m_0} \right) \quad (19)$$

The water-sparing effect of high WUE increases final mass, m , in proportion, if the total mass of water available is fixed as in common competitive conditions. Thus, the increase in r from an increase in WUE is much diluted. If plant B has a 10% advantage over plant A in final mass (a factor of 1.1), then the ratio of relative growth rates is

$$\frac{r_B}{r_A} = \frac{\ln(1.1m/m_0)}{\ln(m/m_0)} = \frac{\ln(1.1) + \ln(m/m_0)}{\ln(m/m_0)} \quad (20)$$

For example, if an annual plant undergoes 10 doublings ($m/m_0 = 1024$), then r_B/r_A is $(0.1 + 6.9)/6.9 = 1.014$, only a 1.4% advantage. The absolute gain remains 10%, and this can be crucial under stress. However, this exercise serves to highlight that exponentially-compounded gains, as in A, are extremely potent. This method of estimating r also assume that one plant's growth is independent of the other's, while commonly there is a further compounding: a gain in r_B for plant B commonly suppresses r_A for plant A, as by mutual shading. A full estimate of final fitness effects requires a full model of concurrent growth.

In any event, one would naturally be led to assign more weight to gains in A than to gains in WUE, PNUE, or $1/f_N$ (frugality in N demand under limited N availability), because gains in A continue to compound until water or N available competitively becomes limiting. It is also worth noting that WUE, while important for competitive water use, is not necessarily related to performance under drought, which is composed variously (Gutschick, 1987) of escape (development outside the dry time), avoidance (access to privileged water sources, as by phreatophytes), tolerance (restricting cellular and developmental damage under a developed stress), and resistance (ability to recover well from such damage). For example, piñon pines have higher WUE than junipers that often grow immediately adjacent (Lajtha and Getz, 1993), but they are far less tolerant of low water potentials (Breshears, unpublished data). It is too simplistic to assume that fitness is related directly to WUE under limitations of water supply, independent of temporal sequence and neighbor relations.

The compounding of the five (or more) performance measures into a measure of fitness and, especially, of relative fit-

ness among species varying in acclimation, is then complex. Nevertheless, it should not be regarded as hopelessly complicated. In biogeographic studies, at a particular site, one may be well aware of the relative value of A versus WUE, for example. The implementation of such judgments extends beyond the scope of the current discussion.

4. Discussion

4.1. Some lessons from the simple models

The combination of carboxylation kinetics, the simple Ball–Berry model of stomatal control, energy balance, and functional balance for N and carbon gains reproduces robust trends that are observed on average in photosynthesis, water-use efficiency, stomatal conductance, and N content. In themselves, the trends are in directions that have long been considered adaptive, in studies of models applied separately from each other, such as stomatal control alone (see, e.g., Cowan and Farquhar, 1977; Farquhar et al., 2002).

This interpretation is only defensible when one does not pay close attention to the great spread in behavior among species, whether this spread be in experimental observations or in simulations. For example, it cannot be adaptive for a species to have a small gain in WUE when other co-occurring species have much greater gains. Nonetheless, the variations in performance and in underlying species-specific acclimations to elevated CO_2 do occur in both the model presented here and in experiments. The range of changes in A predicted here is remarkable, from -6 to $+45\%$ (Fig. 3a). Essentially, the same range is reported by Nowak et al. (2004a,b). Regrettably, it is not straightforward to relate variations in the responses of A to variations in the acclimations used in the model. In the case of *Larrea tridentata*, the lack of significant response in A might be readily related to the decrease in N uptake reported by BassiriRad et al. (2001). There are unfortunately few other cases to date in which both A and root N uptake have been related. In other species, there is the complication that N uptake acclimates in opposite directions in low- and high-N soils (*ibid.*). One more factor that requires attention in comparing modelled and observed responses is that observations often lack a full basis for comparison. For example, assimilation is commonly reported per unit area, but leaf thickness often changes, so that assimilation per unit mass, A_m , can undergo a very different magnitude of change. It is A_m that is most closely related to growth rate (Gutschick, 1987) and that is actually modelled in the present work. No complication is insuperable, but additional data are needed.

More generally, responses to elevated CO_2 , including the acclimations, cannot be expected to be adaptive (Bernacchi et al., 2000; Bunce, 2001; Gutschick and BassiriRad, 2003), given the lack of selection pressure for fitness at high CO_2 for more than 25 million years (Long et al., 2004; critique: Boucot and Gray, 2001). Non- or mal-adaptiveness of responses are seen in resource use (light, N, water, and allocations to acquire these: Bernacchi et al., 2000; Poorter and Nagel, 2000). These are likely to be amplified by maladaptiveness in responses for risk management. An example of risk management is timing of anthesis. It should be early enough to minimize the probability of

plant death and failure of seed-set before frost or drought, and late enough for the plant to use the greatest part of the growth season. Immediate temperature or water status is not a reliable indicator of the risk of premature death, so that plants use surrogate signals of risk, particularly photoperiodic responses. At elevated CO₂ with consequent warming and changed precipitation patterns, the optimal timing and thus the optimal photoperiod length should shift, but there may be inadequate genetic variation to make this shift in the very few generations left before CO₂ doubles or triples (Gutschick and BassiriRad, 2003; Slafer and Rawson, 1996). Other qualifiers to expectations of adaptiveness are readily added. For one, phenotypic changes always must lag in response to evolutionary selection pressures (the Red Queen effect: van Valen, 1973; Stenseth and Maynard Smith, 1984). For another, most changes in traits are nearly neutral in net effect. It may appear, as in the simulations here, that multiple measures of plant performance (A, WUE, etc.) are improved at high CO₂, given the biochemistry and biophysics of today's plants as captured in the four coupled models. However, other performance measures that are not evaluated here (e.g., drought tolerance, cold-hardening) could change in an adverse direction, very nearly cancelling the former gains. This situation of near-neutrality is almost certainly very common (Gutschick and BassiriRad, 2003, esp. pp. 31 ff).

4.2. Implications and ramifications

Fitness patterns in space predict biogeographic distributions, virtually by definition. Predictions of biogeographic shifts among different species, resulting from changes in relative fitness as well as direct disturbance, have become important for many purposes (e.g., Clark et al., 2001). In turn, fitness changes under environmental changes have several key components: (1) autecological shifts, as in resource acquisition and usage efficiencies discussed herein; (2) their compounding in resource competitiveness with other organisms (e.g., Owensby et al., 1999); and (3) biotic interaction shifts, as in relations with pollinators, dispersers, and herbivores (poorly studied: Körner, 2003; Rusterholz and Erhardt, 1998; Veteli et al., 2002).

We may focus on the autecological shifts, leaving the study of their compounding to a useful marriage with community ecology, and the study of biotic shifts to a similar marriage with ecosystem ecology. I have offered the argument here that, as atmospheric CO₂ increases, one may expect considerable diversity among species in the changes in rates and efficiencies of resource use (water, nitrogen, CO₂, light). These predictions are based on a model incorporating key physiological processes and physiological shifts in thermal energy balance. The model is parametrized with data on the diversity of species-specific acclimations in physiological parameters, particularly for uptake of N. The focus here has been on changes in performance of the individual plant, but we should expect changes to propagate to large scales spatially and temporally.

Many observational studies, often mixed with some modelling, are in progress on resource cycles on large spatial scales. Some of these are aimed at detecting current or future changes in fluxes of CO₂, N, or water between land and atmosphere,

with explicit roles for vegetation. Several modelling studies may be considered representative. Luo et al. (1996) focused on photosynthetic enzyme kinetics to predict uniform responses of the carbon cycle across biomes. Bounoua et al. (1999) used more comprehensive physiology and meteorology to estimate changes in surface temperature and evapotranspiration. Their model was run in several modes, allowing separation of indirect effects of elevated CO₂ (radiation balance) and direct or physiological effects. Predicted changes in evapotranspiration and in latitudinal surface-temperature gradients were much reduced by physiological responses, namely, stomatal control and prescribed down-regulation of photosynthetic capacity of two vegetation classes. Rathberger et al. (2003) modelled primary production in pine forests (*Pinus halapensis*) and predicted that direct physiological responses to CO₂ are more important than climatic effects. Dickinson et al. (2002) added to such physiology and meteorology the effects of changes in the nitrogen cycle, using models of root uptake coupled to major N stocks and flows. They did not attempt predictions of changes induced by elevated CO₂; changes in the N cycle processes are yet too variable among species and ecosystems for reliable prediction, as noted here. No climate models yet incorporate rich patterns of physiological acclimation among species or functional groups (if, indeed, the common definitions of functional groups by life form and current patterns of resource use is valid). Intriguingly, Huntingford et al. (2000) used a few-parameter physiological model to predict that species responses to CO₂-induced changes depend strongly on the temperature regime to which they are originally adapted; perhaps functional groups for CO₂ responses need the dimension of temperature adaptation, over and above growth habit and photosynthetic pathway.

Models have also been used in predicting changes in plant distribution under elevated CO₂. Most of these models assign current and future ranges of species or of life zones (e.g., Holdridge) according to spatial patterns of simple temperature measures (T, as means and extremes) and of precipitation (P). Some models use a more dynamic balance of water input with evapotranspiration, estimated by gross physiology (e.g., Woodward and Williams, 1987). The patterns of T and P are observable in the instrumental record; their past values are subject to reconstruction from surrogates, such as isotopic ratios and dendrochronology; their future values are predicted with moderate confidence by climate models, using estimates of the indirect (radiative) effects of elevated CO₂ (but see Visser et al., 2000; Webster et al., 2003 about uncertainties in temperature; Raisanen and Palmer, 2001; Houghton et al., 1990, Fig. 4.11; Dai and Trenberth, 2004 about uncertainties in precipitation). In a few biogeographic models, a limited number of direct physiological effects of CO₂ are incorporated. For example, Solomon and Kirilenko (1997) used the BIOME 1.1 model (Prentice et al., 1992) within their larger model of migration of plant functional types. This model uses photosynthetic parameters and much simplified implicit stomatal control. It does highlight, as do other studies, the problem that potential migration rates of species or life forms may lag well behind rates of movement of climate zones (Kirilenko et al., 2000).

Neither the resource-cycle nor the biogeographic models incorporate the diversity of physiological acclimation to CO₂

among species within plant functional types. The autecological model presented here, however, does not incorporate the tolerance limits of species for temperatures and water status. Neither does the autecological model incorporate the effects of species competition and mutualism, which the common biogeographic models incorporate, though only implicitly (Loehle and LeBlanc, 1996; Vetaas, 2002). There is a clear need to combine these features in improved models for predicting biogeographic changes. Improving the biogeographic models can improve the models of resource cycles, in complementary fashion.

Fundamentally, diversity in patterns of acclimation requires that we add finer resolution to our definitions of plant functional types, grouping of plants by functional group. Diversity, even in one CO₂ response such nitrogen balance, is pronounced within functional groups. The traditional groups are defined by growth forms (Curtis et al., 2003; Medlyn et al., 1999; Poorter and Navas, 2003) or photosynthetic pathway as C₃ versus C₄ (Ghannoum et al., 2000, 2001; Nowak et al., 2004a; Poorter and Navas, 2003; Wand et al., 1999, among others). Diversity in physiological acclimations to CO₂ may not even be predictable by phylogeny; they have not yet been sought by this method, primarily because the diversity has only recently come to our attention. Second, the importance of each performance function varies by habitat and time within a season. The compounded effects on fitness are challenging to evaluate. The net effect of the variations in performance and in their fitness effects is a great dispersion of fitness changes, even within “cohesive” functional groups such as herbaceous C₃ plants, as one case. These variations, if unaccounted, will greatly confound predictions of biogeographic changes. One may term the effect the onset of biogeographic chaos.

4.3. Potential research directions

A more systematic exploration of direct CO₂ effects on fitness and biogeographic distributions appears to be merited, to elucidate changes in plant performance and distribution from the past to the present, as well as to predict changes from the present to the near future. One basic need is a survey of the diversity among species (and genotypes) in the simple control parameters of the basic models used herein— $V_{c,max}$, or, better, the partition function for total leaf N to Rubisco; Ball–Berry parameters m and b or their analogs in other basic stomatal control models; parameters of specific acclimations in m (and b); and the other allocation parameters for root and leaf mass, r and α_L . Frequently, such parameter estimates can be readily extracted from available data. While researchers may be uninterested in their particular studies in, say, fitting g_s behavior to a stomatal control model, the data on g_s and attendant environmental variables plus assimilation rate A are virtually always archived.

To understand patterns, one must examine evolutionary selection regimes, asking which resource is most limiting, how life history strategy affects resource use and competition, etc. It must be admitted that acclimation patterns of some species (e.g., increased N uptake) appear to be particularly adaptive to direct effects of high CO₂. I offer the hypothesis that the apparent adaptiveness is a result of selection pressures that,

in a highly prescribed set of environments, correlate strongly to the indirect effects of CO₂—namely, changed averages and temporal patterns of temperature and precipitation. It is our challenge to elucidate these environments, and the extension to their contrary counterparts that select for responses that are currently maladaptive. In this way, we may understand how the diverse past environments have set the patterns of physiology and biogeography of plant species for the succeeding centuries. The ultimate application might be the spatial mapping of areas according to: (1) the relative importance, in interplant competitive status, of A, N economy ($1/f_N$), PNUE, WUE, and water-use rate (effectively, g_s), which are the variables simulated herein; (2) observed trends in species abundance, particularly if they can be related to these five (or more) performance measures; and (3) determination of genetic linkages among traits for the direct and indirect effects of CO₂, extending to measurements of selection coefficients on acclimation traits, wherever this is feasible.

The simple composite model presented here merits extension. We have proposed accounting for mycorrhizal roles in C and N economies in plants at elevated CO₂ (BassiriRad et al., 2001). Changes in stomatal sensitivity to humidity, water stress, and CO₂ itself (Urban, 2003) can be accounted, by modifying the Ball–Berry model. I have used here only one possible form of this modification. The models must also be merged with other models that account for the indirect CO₂ effects, that is, the shifts in temperature and precipitation regimes. The roles of extremes in these climatic variables need attention, too. Common biogeographic models consider very simple statistics in driving variables, rather than in the state of the organisms themselves (Gutschick and BassiriRad, 2003). Tolerance of extreme high and low temperatures has been shown to change under high CO₂ (Hamerlynck et al., 2000; Lutze et al., 1998). Accounting must be added for nonsteady availability of resources. Interruption of water supplies by drought induces acclimations of stomatal conductance, photosynthetic capacity, and N uptake that do not “average out” to the steady-state acclimations—e.g., reduced stomatal conductance persists for varying times (Loewenstein and Pallardy, 2002). On longer time scales, episodic drought years or N additions or losses perturb the tendency of ecosystems to reach co-limitation such as that seen in equilibrating leaf area development to long-term water supply (Kergoat, 1998). Similarly, “sudden” changes of CO₂ over several years perturb soil N availability, limiting plant growth gains for what are likely to be extended times (Körner, 2003; Nowak et al., 2004a, Fig. 9 therein).

These extensions of the model should be pursued within one general model with parameter values introduced for each species or genotype, in contrast to unique models for each species. This is in the spirit of a recent successful study of biodiversity as affected by climate but not by direct CO₂ effects (Kleidon and Mooney, 2000). Finally, attention must be paid to composing fitness functions to predict population shifts, accounting for the spectrum of limiting factors at a site and their unique weighting in the life history strategy of each species. In this manner, we may deduce more useful predictions or hypotheses, unsettling though they may be, about the rise of CO₂ in what has been described as our global uncontrolled experiment (Revelle and Seuss, 1957; Baes et al., 1977).

Acknowledgments

The author gratefully acknowledges the support of the Jornada Long-Term Ecological Research Program (NSF grant DEB-00R0412) and a wealth of discussions with students and colleagues over the years. Two anonymous reviews provided valuable comments, including the suggestion to explore more complete models, which proved to modify the conclusions significantly.

Appendix A

A number of commonly observed trends in plant performance may be demonstrated semi-quantitatively with model simplifications. One example is modelling how g_s might track photosynthetic capacity. In the Ball-Berry model (Eq. (3)), let us drop the small intercept, b . Let us also express the photosynthetic rate in terms of C_i , thereby lumping together the mesophyll liquid-phase conductance and the enzyme kinetics as an effective mesophyll conductance, g_m . This makes g_m the slope of A versus C_i in a linearized model. We may write

$$A = g_m \frac{C_i}{P} \tag{A1}$$

Fig. 5a applies this linearization to data of Niinemets et al. (1998) on two forest trees. The upper curve is for a leaf of fast-growing *Populus tremula*, the lower is for a more shaded leaf of slow-growing *Tilia cordata*. The slope (g_m) has been chosen to make the curve pass through the normal (unstressed) operating point of each leaf, in which C_i is approximately $0.7 \times C_a$, or 25.9 Pa. Note that linearity holds well on going to lower C_i , but poorly on going to higher C_i ; the linear model with zero intercept has a limited range of applicability.

Now consider the expression for A in terms of CO_2 transport through the stomata,

$$A = g'_s \frac{(C_a - C_i)}{P} \tag{A2}$$

Here, g'_s is the stomatal conductance for CO_2 , which is 0.62 times as large as that for water vapor (g_s , not superscripted). We ignore the large boundary-layer conductance (at some peril; see Fig. 4). We can equate the two rates, obtaining a relation for C_i :

$$C_i = C_a \frac{g'_s}{(g'_s + g_m)} \tag{A3}$$

We can substitute Eq. (A3) into Eq. (A1), obtaining an expression for A in terms of the ambient CO_2 concentration and the two conductances,

$$A = \frac{C_a}{P} \frac{g'_s g_m}{(g'_s + g_m)} \tag{A4}$$

Fig. 5b applies the relation of Eq. (A2) to the data of Niinemets et al. (1998), creating a “load line” as it is commonly called. Each load line is specific to a choice of stomatal conductance. The intersection of the load line with the

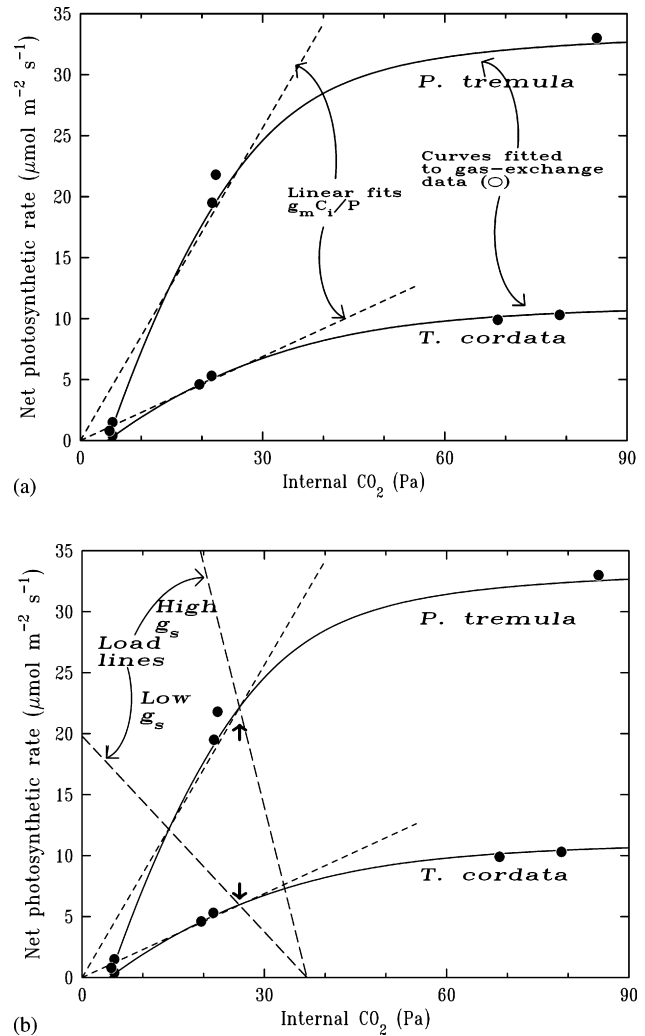


Fig. 5 – Use of linear approximation for enzyme-kinetic photosynthetic response to internal CO_2 (Eq. (A1)) to estimate dependence of assimilation rate A upon effective mesophyll conductance, g_m , and stomatal conductance, g_s : (a) construction of g_m as slope of line passing through current operating point of plant at $0.7 \times C_a = 25.9$ Pa, using data of Niinemets et al. (1998) for sun-tolerant *Populus tremula* and shade-tolerant *Tilia cordata*. (b) Estimation of C_i and A corresponding to two different values of g_s . Load lines represent transport relation, Eq. (A2). Upper and lower curves are respectively for $g_s = 0.20$ and $0.054 \text{ mol m}^{-2} \text{ s}^{-1}$. Intersection of load lines with linear or actual curves for enzyme-kinetic relation gives value of C_i that satisfies both the transport and enzyme-kinetic equations.

enzyme-kinetic curve or a linear approximation to this curve (i.e., Eq. (A1)) determines the operating point, C_i . This geometric construction demonstrates visually the effects of changing g'_s (or changing g_m) upon C_i . The higher load line is for $g'_s = 0.20 \text{ mol m}^{-2} \text{ s}^{-1}$, which is normal for *P. tremula*. The lower line is for $g'_s = 0.054 \text{ mol m}^{-2} \text{ s}^{-1}$, normal for *T. cordata*. If *P. tremula* undergoes a shift to the lower value of g'_s , such as from stress, C_i shifts downward by almost one-half, and A decreases similarly. If *T. cordata* experiences a large increase

in g'_s , to the high value that is normal for *P. tremula*, the shift in C_i is more modest, about 25%, and so, too, is the shift in A . These contrasting effects are captured in Eq. (A3). We may also consider changes in g_m , such as occur from differences in nitrogen nutrition; these scale all the curves of A versus C_i up or down. One may use the equations or the geometric constructions to examine these effects.

To examine how g'_s and g_m are coordinated, we insert this into the Ball–Berry equation, again, dropping the intercept b , to get

$$g_s = m \frac{(C_a/P)0.62g_s g_m h_s}{(C_s/P)(0.62g_s + g_m)} \quad (A5)$$

The value of C_s is very nearly that of C_a when boundary-layer conductance is large, so we may cancel the first terms in parentheses in the numerator and denominator. We may also cancel g_s between the left side (which now become unity) and the right side. Finally, we move the factor $(0.62g_s + g_m)$ to the left side, obtaining

$$0.62g_s + g_m = 0.62m h_s g_m \quad (A6)$$

Bringing the two terms in g_m together on the right-hand side and multiplying both sides by $1.6 = 1/0.62$, we finally obtain

$$g_s = g_m(mh_s - 1.6) \quad (A7)$$

This is a remarkable, if approximate, relation. It indicates that g_s is “paced” to photosynthetic capacity, recalling the classic experiments of Wong et al. (1985a,b,c). It indicates that g_s decreases if humidity decreases (that is, if vapor pressure deficit increases). It also indicates that g_s does not respond to CO_2 levels other than by changes in g_m . Other common models of stomatal behavior with separable humidity responses (Leuning, 1995; Dewar, 1995) give exactly analogous results: there is no significant shift of g_s without down-regulation of nitrogen content.

The linear relation of g_s to the product of m and h_s is evident in experimental data. Fig. 6 shows the “intrinsic” response of g_s to h_s , factoring out the feedback of g_s on A and back to g_s (Gutschick and Simonneau, 2002 offer some review of this concept). This is achieved by computing the quantity $g_s A/C_s$ in the Ball–Berry relation. Such calculations on data of Bunce (1993) on soybeans, *Glycine max*, show a linear relation. However, the slope and intercept are not preserved between conditions of growth or measurement at different CO_2 concentrations, as a comparison of the three curves demonstrates. Eq. (A7) is only an approximation, useful for initial estimates.

This brings us to the final sub-model that predicts adaptive acclimation in nitrogen content ... but, again, there is another interesting inference about water-use efficiency from the stomatal control model.

Water-use efficiency, WUE, or W , is defined as the ratio between photosynthetic gain and water loss. The gain and the loss can be computed on a variety of bases. For example, gain can be taken as gross photosynthesis, or as net photosynthesis after respiratory losses, or as final dry matter, including leaf loss, etc. A simple measure is the ratio of photosynthetic

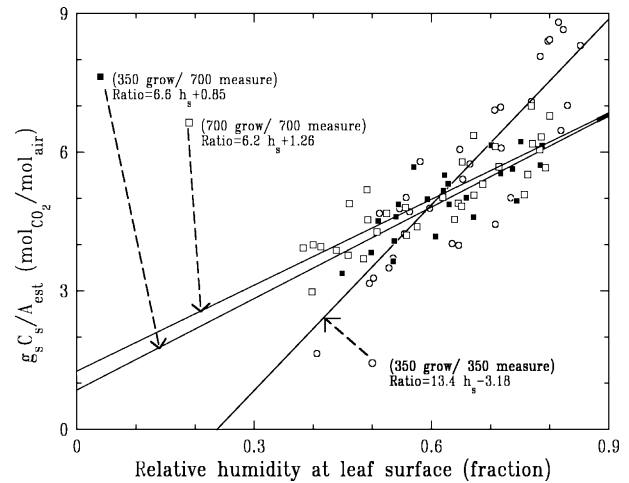


Fig. 6 – Estimation of intrinsic response of stomatal conductance, g_s , to surface relative humidity, h_s , as slope of the regression of $g_s C_s/A$ (“Ratio”, in legend) vs. h_s . Data of Bunce (1993) on soybeans, *Glycine max*, refer to three different combinations of CO_2 for growth (350 or 700 mol mol⁻¹) and measurement.

CO_2 assimilation to transpiration at the leaf, $W = A/E$. Here, E is the transpiration rate per leaf area. Consistent with ignoring the leaf boundary layer to date, this is approximated as g_s multiplied by the water vapor deficit, D , which is the difference of water vapor pressure from leaf interior to ambient air, $e_i - e_a$. The magnitude of e_i is very closely the saturated vapor pressure at leaf temperature, $e_s(T_L)$. The magnitude of e_a is the saturated vapor pressure at air temperature, multiplied by the relative humidity (as a fraction). When the leaf is near air temperature, the two saturated vapor pressures are similar, and we may approximate D as

$$D = e_s(T)(1 - h_s) \quad (A8)$$

The relative humidity is the same as that in Eqs. (2) and (A5)–(A7).

Now we may develop good approximate expressions for water-use efficiency:

$$W = \frac{g'_s(C_a - C_i)}{g_s(e_i - e_a)} = \frac{0.62C_a(1 - C_i/C_a)}{e_s(1 - h_s)} \quad (A9)$$

This common form alone emphasizes features of the control of W ; it rises with ambient CO_2 , falls with increasing temperature (which raises e_s), rises with h_s , and falls with an increase in C_i/C_a . The last factor is under physiological control and is estimated experimentally from the stable isotopic composition of plant sugars or tissues (Farquhar et al., 1982; Farquhar and Richards, 1984). It can be estimated in our simple model set by rearranging Eq. (A3). We can go further, using Eq. (A7) to express g_s in terms of g_m (or the reverse), which yields

$$\frac{C_i}{C_a} \approx \frac{1.6}{mh_s} \Rightarrow W = \frac{C_a}{me_s h_s(1 - h_s)} \quad (A10)$$

Several remarkable features are (a) that C_i/C_a is determined essentially only by (i) the Ball–Berry slope, m , which is a stomatal feedback parameter, and not by photosynthetic capacity at all, to this approximation and (ii) relative humidity, h_s ; (b) that water-use efficiency rises in direct proportion to ambient CO_2 , falls in inverse proportion to Ball–Berry slope, falls exponentially with temperature (because e_s rises exponentially), and has a minimum at the intermediate relative humidity of $h_s = 0.5 = 50\%$. At both extremes of high and low humidity, W is high—either by suppression of the vapor pressure deficit at high humidity or by stomatal restriction that reduces C_i/C_a at low humidity. Fig. 7 shows a test of the predicted nearly-parabolic relation of W to h_s , again using data of Bunce (1993). The particular prediction of a minimum in W at intermediate humidities is supported in part; there are few experimental data at very low h_s to test the rise of W here. Note that there is an implied cutoff of g_s at a finite h_s near 0.3, for plants raised and measured at normal CO_2 levels; this is evident in the original data of Bunce (1993, Fig. 1 therein).

Fig. 8 shows the application of Eq. (A10), with some modification, to a complete canopy of pecan, *Carya illinoensis*. Eddy covariance was used to measure water and CO_2 fluxes in an irrigated orchard in Las Cruces, New Mexico, USA (Andales et al., 2006). The values of monthly-total W computed from the data were used in a linear regression against the quantity $(1 - R_d/A)/[e_{sat}(T)h_r(1-1.23h_r)]$. This is similar to the right-hand

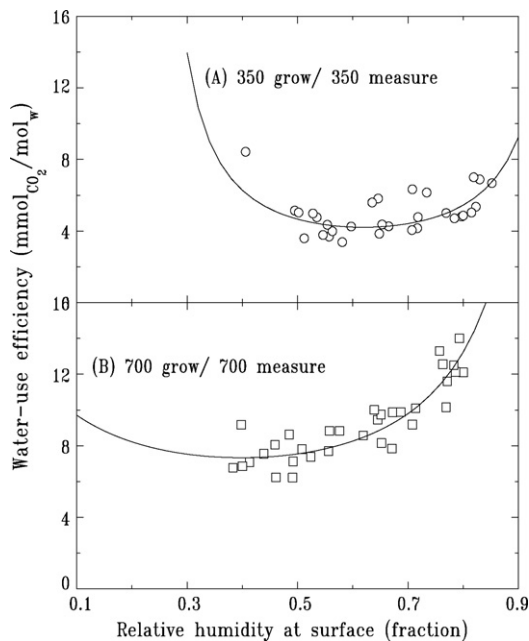


Fig. 7 – Estimation of dependence of water-use efficiency, A/E , upon relative humidity at leaf surface in soybeans, *Glycine max* (data of Bunce, 1993). Assimilation, A , is estimated from regression of A against h_s in original data. Transpiration, E , is computed from transport equation (Eq. (7), without the factor λ for conversion to energy flux density), with g_s estimated from Ball–Berry equation (Eq. (3)) and regression lines in Fig. 6. Two response curves differ in CO_2 mixing ratios used in both growth and measurement, as indicated in $mol\ mol^{-1}$. Solid line is prediction from Eq. (A10) with $m = 10$ and published leaf temperature of $30^\circ C$.

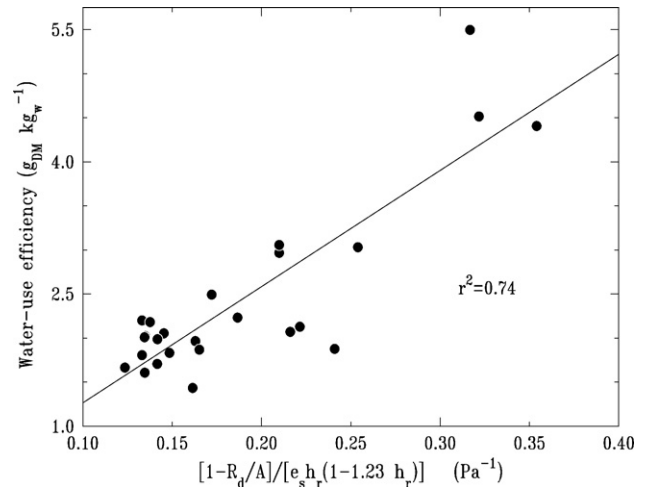


Fig. 8 – Estimation of dependence of monthly-total water-use efficiency, A/E , upon relative humidity in free air in a closed canopy of irrigated pecan trees, *Carya illinoensis*, in year 2002. Both A and E were derived by eddy-covariance measurements above the canopy (Miller et al., submitted for publication). Predictor variable is a modification of that in Eq. (A10), corrected for: (a) ecosystem respiration, R_d , estimated from nocturnal CO_2 flux scaled to temperature at all other times of day and (b) more complete model of response of C_i/C_a (Eq. (A9)) to humidity; see text for details.

side of Eq. (A10). The added factor $1 - R_d/A$ corrects approximately for respiratory losses, R_d , effectively converting results to instantaneous W of all leaves taken together. The magnitude of R_d was estimated for nighttime conditions and extrapolated to daytime conditions as an exponential form in temperature. Leaf surface humidity, h_s , was not measurable, so that relative humidity in air, h_r , was used. Finally, $1 - h_r$ was replaced by $1 - 1.23h_r$, using results of the complete model used in the main text here. This replacement moderately improved the accuracy of the fit (original $r^2 = 0.70$). The simple model is still of limited accuracy. The limitation is more pronounced when one excludes data from months early and late in the growing season, when W is high. These extreme values dominate the least-squares fit.

These relations are, it must be noted, approximate. They are modulated by several things, including the approximate nature of the Ball–Berry formula, the neglect of the boundary layer effect, and by the effect of stomatal restriction on transpirational cooling that lowers leaf T and raises W .

REFERENCES

- Andales, A., Wang, J.M., Sammis, T.W., Mexal, J.G., Simmons, L.J., Miller, D.R., Gutschick, V.P., 2006. A model of pecan tree growth for the management of pruning and irrigation. *Agric. Water Management* 84, 77–88.
- Atkin, O.K., Holly, C., Ball, M.C., 2000. Acclimation of snow gum (*Eucalyptus pauciflora*) leaf respiration to seasonal and diurnal variations in temperature: the importance of changes in the capacity and temperature sensitivity of respiration. *Plant Cell Environ.* 23, 15–26.

- Baer, C.F., Goeller, H.E., Olson, J.S., Rotty, R.M., 1977. Carbon dioxide and climate: the uncontrolled experiment. *Am. Scientist* 65, 310–320.
- Ball, J.T., Woodrow, I.E., Berry, J.A., 1987. A model predicting stomatal conductance and its contribution to the control of photosynthesis under different environmental conditions. In: Biggins, J. (Ed.), *Progress in Photosynthesis Research*, vol. 4. M Nijhoff, Dordrecht, pp. 221–224.
- BassiriRad, H., Gutschick, V.P., Lussenhop, J., 2001. Root system adjustments: regulation of plant nutrient uptake and growth responses to elevated CO₂. *Oecologia* 126, 305–320.
- Bell, C.J., 1982. A model of stomatal control. *Photosynthetica* 16, 486–495.
- Bernacchi, C.J., Coleman, J.S., Bazzaz, F.A., McConnaughay, K.D.M., 2000. Biomass allocation in old-field annual species grown in elevated CO₂ environments: no evidence for optimal partitioning. *Global Change Biol.* 6, 855–863.
- Beyschlag, W., Barnes, P.W., Ryel, R., Caldwell, M.M., Flint, S.D., 1990. Plant competition for light analyzed with a multispecies canopy model. 2. Influence of photosynthetic characteristics on mixtures of wheat and wild oat. *Oecologia* 82, 374–380.
- Boucot, A.J., Gray, J., 2001. A critique of Phanerozoic climatic models involving changes in the CO₂ content of the atmosphere. *Earth Sci. Rev.* 56, 1–159.
- Bounoua, L., Collatz, G.J., Sellers, P.J., Randall, D.A., Dazlich, D.A., Los, S.O., Berry, J.A., Fung, I., Tucker, C.J., Field, C.B., Jensen, T.G., 1999. Interactions between vegetation and climate: radiative and physiological effects of doubled atmospheric CO₂. *J. Climate* 12, 309–324.
- Buffington, L.C., Herbel, C.H., 1965. Vegetational changes on a semidesert grassland range from 1858 to 1963. *Ecol. Monogr.* B35, 139–164.
- Bunce, J.A., 1993. Effects of doubled atmospheric carbon dioxide concentrations on the responses of assimilation and conductance to humidity. *Plant Cell Environ.* 16, 189–197.
- Bunce, J.A., 1998. Effects of environment during growth on the sensitivity of leaf conductance to changes in humidity. *Global Change Biol.* 4, 269–274.
- Bunce, J.A., 2001. Are annual plants adapted to the current atmospheric concentration of carbon dioxide? *Int. J. Plant Sci.* 162, 1261–1266.
- Caldwell, M.M., Meister, H.P., Tenhunen, J.D., Lange, O.L., 1986. Canopy structure, light microclimate, and leaf gas exchange of *Quercus coccifera* L. in a Portuguese *macchia*: measurements in different canopy layers and simulations with a canopy model. *Trees* 1, 25–41.
- Clark, J.S., Carpenter, S.R., Barber, M., Collins, S., Dobson, A., Foley, J.A., Lodge, D.M., Pascual, M., Pielke, R., Pizer, W., 2001. Ecological forecasts: an emerging imperative. *Science* 293, 657–660.
- Collatz, G.J., Ball, J.T., Grivet, C., Berry, J.A., 1991. Physiological and environmental regulation of stomatal conductance, photosynthesis and transpiration: a model that includes a laminar boundary layer. *Agric. For. Meteorol.* 54, 107–136.
- Collatz, G.J., Ribascarbo, M., Berry, J.A., 1992. Coupled photosynthesis–stomatal conductance model for leaves of C₄ plants. *Aust. J. Plant Physiol.* 19, 519–538.
- Cowan, I.R., Farquhar, G.D., 1977. Stomatal diffusion in relation to leaf metabolism and environment. *Symp. Soc. Exper. Biol.* 31, 471–505.
- Curtis, P.S., Jablonski, L.M., Wang, X.Z., 2003. Assessing elevated CO₂ responses using meta-analysis. *New Phytol.* 160, 6–7.
- Dai, A., Trenberth, K.E., 2004. The diurnal cycle and its depiction in the Community Climate System Model. *J. Climate* 17, 930–951.
- Day, W., Chalabi, Z.S., 1988. Use of models to investigate the link between the modification of photosynthetic characteristics and improved crop yields. *Plant Physiol. Biochem.* 26, 511–517.
- de Pury, D.D.G., Farquhar, G.D., 1997. Simple scaling of photosynthesis from leaves to canopies without the errors of big-leaf models. *Plant Cell Environ.* 20, 537–557.
- Dewar, R.C., 1995. Interpretation of an empirical model for stomatal conductance in terms of guard cell function: theoretical paper. *Plant Cell Environ.* 18, 365–372.
- Dewar, R.C., 2002. The Ball–Berry–Leuning and Tardieu–Davies stomatal models: synthesis and extension within a spatially aggregated picture of guard cell function. *Plant Cell Environ.* 25, 1383–1398.
- Dickinson, R.E., Berry, J.A., Bonan, G.B., Collatz, G.J., Field, C.B., Fung, I.Y., Goulden, M., Hoffmann, W.A., Jackson, R.B., Myneni, R., Sellers, P.J., Shaikh, M., 2002. Nitrogen controls on climate model evapotranspiration. *J. Climate* 15, 278–295.
- Ehleringer, J.R., Cerling, T.E., Dearing, M.D., 2002. Atmospheric CO₂ as a global change driver influencing plant–animal interactions. *Integr. Comp. Biol.* 42, 424–430.
- Ellsworth, D.S., 1999. CO₂ enrichment in a maturing pine forest: are CO₂ exchange and water status in the canopy affected? *Plant Cell Environ.* 22, 461–472.
- Farquhar, G.D., von Caemmerer, S., Berry, J.A., 1980. A biochemical model of photosynthetic CO₂ assimilation in leaves of C₃ species. *Planta* 149, 78–90.
- Farquhar, G.D., O’Leary, M.H., Berry, J.A., 1982. On the relationship between carbon isotope discrimination and the intercellular carbon dioxide concentration in leaves. *Aust. J. Plant Physiol.* 9, 121–137.
- Farquhar, G.D., Richards, R.A., 1984. Isotopic composition of plant carbon correlates with water use efficiency of wheat genotypes. *Aust. J. Plant Physiol.* 11, 539–552.
- Farquhar, G.D., Buckley, T.N., Miller, J.M., 2002. Optimal stomatal control in relation to leaf area and nitrogen content. *Silva Fennica* 36, 625–637.
- Field, C., Mooney, H.A., 1986. The photosynthesis–nitrogen relationship in wild plants. In: Givnish, T.J. (Ed.), *On the Economy of Plant Form and Function*. Cambridge University Press, Cambridge, pp. 25–55.
- Friedlingstein, P., Joel, G., Field, C.B., Fung, I.Y., 1999. Toward an allocation scheme for global terrestrial carbon models. *Global Change Biol.* 5, 755–770.
- Futuyma, D., 1998. *Evolutionary Biology*, 3rd ed. Sinauer, Sunderland, MA, USA.
- Ghannoum, O., von Caemmerer, S., Ziska, L.H., Conroy, J.P., 2000. The growth response of C₄ plants to rising atmospheric CO₂ partial pressure: a reassessment. *Plant Cell Environ.* 23, 931–942.
- Ghannoum, O., von Caemmerer, S., Conroy, J.P., 2001. Plant water use efficiency of 17 Australian NAD-ME and NADP-ME C₄ grasses at ambient and elevated CO₂ partial pressure. *Aust. J. Plant Physiol.* 28, 1207–1217.
- Goverde, M., Arnone, J.A., Erhardt, A., 2002. Species-specific reactions to elevated CO₂ and nutrient availability in four grass species. *Basic Appl. Ecol.* 3, 221–227.
- Gutschick, V.P., 1987. *A Functional Biology of Crop Plants*. Croom Helm, London/Timber Press, Beaverton, OR.
- Gutschick, V.P., BassiriRad, H., 2003. Extreme events as shaping physiology, ecology, and evolution of plants: toward a unified definition and evaluation of their consequences. *New Phytol.* 160, 21–42.
- Gutschick, V.P., Kay, L.E., 1995. Nutrient-limited growth rates: quantitative benefits of stress responses and some aspects of regulation. *J. Exp. Bot.* 46, 995–1009.
- Gutschick, V.P., Simonneau, T., 2002. Modelling stomatal conductance of field-grown sunflower under varying soil water content and leaf environment: comparison of three models of stomatal response to leaf environment and coupling with an abscisic acid-based model of stomatal response to soil drying. *Plant Cell Environ.* 25, 1423–1434.

- Hamerlynck, E.P., Huxman, T.E., Loik, M.E., Smith, S.D., 2000. Effects of extreme high temperature, drought and elevated CO₂ on photosynthesis of the Mojave Desert evergreen shrub *Larrea tridentata*. *Plant Ecol.* 148, 183–193.
- Houghton, J.T., Jenkins, G.J., Ephraim, J.J., 1990. *Climate Change: The IPCC Assessment*. Cambridge University Press, Cambridge.
- Huntingford, C., Cox, P.M., Lenton, T.M., 2000. Contrasting responses of a simple terrestrial ecosystem model to global change. *Ecol. Mod.* 134, 41–48.
- Huxman, T.E., Smith, S.D., 2001. Photosynthesis in an invasive grass and native forb at elevated CO₂ during an El Niño year in the Mojave Desert. *Oecologia* 128, 193–201.
- Kergoat, L., 1998. A model for hydrological equilibrium of leaf area index on a global scale. *J. Hydrol.* 213, 268–286.
- Kimura, M., 1983. *The Neutral Theory of Molecular Evolution*. Cambridge University Press, New York, USA.
- Kirilenko, A.P., Belotelov, N.V., Bogatyrev, B.G., 2000. Global model of vegetation migration: incorporation of climatic variability. *Ecol. Mod.* 132, 125–133.
- Kleidon, A., Mooney, H.A., 2000. A global distribution of biodiversity inferred from climatic constraints: results from a process-based modelling study. *Global Change Biol.* 6, 507–523.
- Körner, C., 2001. Experimental plant ecology: some lessons from global change research. In: Press, M.C., et al. (Eds.), *Ecology: Achievement and Challenge*. Oxford University Press, Oxford, pp. 227–247.
- Körner, C., 2003. Ecological impacts of atmospheric CO₂ enrichment on terrestrial ecosystems. *Philos. Trans. R. Soc.* A361, 2023–2041.
- Lajtha, K., Getz, J., 1993. Photosynthesis and water-use efficiency in pinyon-juniper communities along an elevation gradient in northern New Mexico. *Oecologia* 94, 95–101.
- Leuning, R., 1990. Modelling stomatal behaviour and photosynthesis of *Eucalyptus grandis*. *Aust. J. Plant Physiol.* 17, 159–175.
- Leuning, R., 1995. A critical appraisal of a combined stomatal-photosynthesis model for C₃ plants. *Plant Cell Environ.* 4, 339–355.
- Loehle, C., LeBlanc, D., 1996. Model-based assessments of climate change effects on forests: a critical review. *Ecol. Mod.* 90, 1–31.
- Loewenstein, N.J., Pallardy, S.G., 2002. Influence of a drying cycle on post-drought xylem sap abscisic acid and stomatal responses in young temperate deciduous angiosperms. *New Phytol.* 156, 351–361.
- Long, S.P., Ainsworth, E.A., Rogers, A., Ort, D.R., 2004. Rising atmospheric carbon dioxide: plants face the future. *Annu. Rev. Plant Biol.* 55, 591–628.
- Luo, Y., Sims, D.A., Thomas, R.B., Tissue, D.T., Ball, J.T., 1996. Sensitivity of leaf photosynthesis to CO₂ concentration is an invariant function for C₃ plants: a test with experimental data and global applications. *Global Biogeochem. Cycles* 10, 209–222.
- Lutze, J.L., Roden, J.S., Holly, C.J., Wolfe, J., Egerton, J.J.G., Ball, M.C., 1998. Elevated atmospheric CO₂ promotes frost damage in evergreen tree seedlings. *Plant Cell Environ.* 21, 631–635.
- Medlyn, B.E., Badeck, F.W., De Pury, D.G.G., Barton, C.V.M., Broadmeadow, M., Ceulemans, R., De Angelis, P., Forstreuter, M., Jach, M.E., Kellomaki, S., Laitat, E., Marek, M., Philippot, S., Rey, A., Strassmeyer, J., Laitinen, K., Liozon, R., Portier, B., Roberntz, P., Wang, K., Jarvis, P.G., 1999. Effects of elevated [CO₂] on photosynthesis in European forest species: a meta-analysis of model parameters. *Plant Cell Environ.* 22, 1475–1495.
- Miller, D.R., Sammis, T.W., Simmons, L.J., Gutschick, V.P., Wang, J. Measurement and simple model for pecan water use efficiency. *Agric. Water Manage.*, submitted for publication.
- Morison, J.I.L., 1998. Stomatal response to increased CO₂ concentration. *J. Exp. Bot.* 49, 443–452.
- Mott, K.A., 1988. Do stomata respond to CO₂ concentrations other than intercellular? *Plant Physiol.* 86, 200–203.
- Navas, M.L., Sonie, L., Richarte, J., Roy, J., 1997. The influence of elevated CO₂ on species phenology, growth and reproduction in a Mediterranean old-field community. *Global Change Biol.* 3, 523–530.
- Niinemets, Ü., Kull, O., Tenhunen, J.D., 1998. An analysis of light effects on foliar morphology, physiology, and light interception in temperature deciduous woody species of contrasting shade tolerance. *Tree Physiol.* 18, 681–696.
- Niinemets, Ü., Sober, A., Kull, O., Hartung, W., Tenhunen, J.D., 1999. Apparent controls on leaf conductance by soil water availability and via light-acclimation of foliage structural and physiological properties in a mixed deciduous, temperate forest. *Int. J. Plant Sci.* 160, 707–721.
- Nowak, R.S., Ellsworth, D.S., Smith, S.D., 2004a. Functional responses of plants to elevated atmospheric CO₂—do photosynthetic and productivity data from FACE experiments support early predictions? *New Phytol.* 162, 253–280.
- Nowak, R.S., Zitzer, S.F., Babcock, D., Smith-Longozo, V., Charlet, T.N., Coleman, J.S., Seemann, J.R., Smith, S.D., 2004b. Elevated atmospheric CO₂ does not conserve soil water in the Mojave Desert. *Ecology* 85, 93–99.
- Owensby, C.E., Ham, J.M., Knapp, A.K., Auen, L.M., 1999. Biomass production and species composition change in a tallgrass prairie ecosystem after long-term exposure to elevated atmospheric CO₂. *Global Change Biol.* 5, 497–506.
- Pearson, P.N., Palmer, M.R., 2000. Atmospheric carbon dioxide concentrations over the past 60 million years. *Nature* 406, 695–699.
- Polley, H.W., Johnson, H.B., Tischler, C.R., 2003. Woody invasion of grasslands: evidence that CO₂ enrichment indirectly promotes establishment of *Prosopis glandulosa*. *Plant Ecol.* 164, 85–94.
- Poorter, H., Nagel, O., 2000. The role of biomass allocation in the growth response of plants to different levels of light, CO₂, nutrients and water: a quantitative review. *Aust. J. Plant Physiol.* 27, 595–607.
- Poorter, H., Navas, M.L., 2003. Plant growth and competition at elevated CO₂: on winners, losers and functional groups. *New Phytol.* 157, 175–198.
- Prentice, I.C., Cramer, W.P., Harrison, S.P., Leemans, R., Monserud, R.A., Solomon, A.M., 1992. A global biome model based on plant physiology and dominance, soil properties and climate. *J. Biogeogr.* 19, 117–134.
- Pritchard, S.G., Rogers, H.H., Prior, S.A., Peterson, C.M., 1999. Elevated CO₂ and plant structure: a review. *Global Change Biol.* 5, 807–837.
- Raisanen, J., Palmer, T.N., 2001. A probability and decision-model analysis of a multimodel ensemble of climate change simulations. *J. Climate* 14, 3212–3226.
- Rathberger, C., Nicault, A., Kaplan, J.O., Guiot, J., 2003. Using a biogeochemistry model in simulating forests productivity responses to climatic change and CO₂ increase: example of *Pinus halapensis* in Provence (southeast France). *Ecol. Mod.* 166, 239–255.
- Reekie, E.G., Bazzaz, F.A., 1991. Phenology and growth in 4 annual species grown in ambient and elevated CO₂. *Can. J. Bot. Rev. Can. Bot.* 69, 2475–2481.
- Revelle, R., Seuss, H.E., 1957. Carbon dioxide exchange between atmosphere and ocean and the question of an increase of atmospheric CO₂ during the past decades. *Tellus* 9, 18–27.
- Rusterholz, H.P., Erhardt, A., 1998. Effects of elevated CO₂ on flowering phenology and nectar production of nectar plants important for butterflies of calcareous grasslands. *Oecologia* 113, 341–349.
- Santrucek, J., Sage, R.F., 1996. Acclimation of stomatal conductance to a CO₂-enriched atmosphere and elevated temperature in *Chenopodium album*. *Aust. J. Plant Physiol.* 23, 467–478.

- Schultz, H., Lebon, E., 1995. Modelling vineyard transpiration and assimilation under water limiting conditions. In: 3eme Rapport d'Avancement des Travaux. INRA, Montpellier, France.
- Sinclair, T.J., Horie, T., 1989. Leaf nitrogen, photosynthesis, and crop radiation use efficiency: a review. *Crop. Sci.* 29, 90–98.
- Slafer, G.A., Rawson, H.M., 1996. Responses to photoperiod change with phenophase and temperature during wheat development. *Field Crops Res.* 46, 1–13.
- Solomon, A.M., Kirilenko, A.P., 1997. Climate change and terrestrial biomass: what if trees do not migrate? *Global Ecol. Biogeogr. Lett.* 6, 139–148.
- Stenseth, N.C., Maynard Smith, J., 1984. Coevolution in ecosystems: Red Queen or stasis? *Evolution* 38, 870–880.
- Stulen, I., Den Hertog, J., 1993. Root growth and functioning under atmospheric CO₂ enrichment. *Vegetatio* 104, 99–115.
- Tuzet, A., Perrier, A., Leuning, R., 2003. A coupled model of stomatal conductance, photosynthesis and transpiration. *Plant Cell Environ.* 26, 1097–1116.
- Urban, O., 2003. Physiological impacts of elevated CO₂ concentration ranging from molecular to whole plant responses. *Photosynthetica* 41, 9–20.
- van Noordwijk, M., Martikainen, P., Bottner, P., Cuevas, E., Rouland, C., Dhillon, S.S., 1998. Global change and root function. *Global Change Biol.* 4, 759–772.
- van Oosten, J.J., Besford, R.T., 1995. Some relationships between the gas-exchange biochemistry and molecular biology of photosynthesis during leaf development of tomato plants after transfer to different carbon dioxide concentrations. *Plant Cell Environ.* 18, 1253–1266.
- van Valen, L., 1973. A new evolutionary law. *Evol. Theory* 1, 1–30.
- Vetaas, O.R., 2002. Realized and potential climate niches: a comparison of four *Rhododendron* tree species. *J. Biogeogr.* 29, 545–554.
- Veteli, T.O., Kuokkanen, K., Julkunen-Tiitto, R., Roininen, H., Tahvanainen, J., 2002. Effects of elevated CO₂ and temperature on plant growth and herbivore defensive chemistry. *Global Change Biol.* 8, 1240–1252.
- Visser, H., Folkert, R.J.M., Hoekstra, J., De Wolff, J.J., 2000. Identifying key sources of uncertainty in climate change projections. *Clim. Change* 45, 421–457.
- Wand, S.J.E., Midgley, G.F., Jones, M.H., Curtis, P.S., 1999. Responses of wild C₄ and C₃ grass (*Poaceae*) species to elevated atmospheric CO₂ concentration: a meta-analytic test of current theories and perceptions. *Global Change Biol.* 5, 723–741.
- Ward, J.K., Kelly, J.K., 2004. Scaling up evolutionary responses to elevated CO₂: lessons from *Arabidopsis*. *Ecol. Lett.* 7, 427–440.
- Ward, J.K., Strain, B.R., 1997. Effects of low and elevated CO₂ partial pressure on growth and reproduction of *Arabidopsis thaliana* from different elevations. *Plant Cell Environ.* 20, 254–260.
- Webster, M., Forest, C., Reilly, J., Babiker, M., Kicklighter, D., Mayer, M., Prinn, R., Sarofim, M., Sokolov, A., Stone, P., Wang, C., 2003. Uncertainty analysis of climate change and policy response. *Clim. Change* 61, 295–320.
- Wong, S.-C., Cowan, I.R., Farquhar, G.D., 1985a. Leaf conductance in relation to rate of CO₂ assimilation. 1. Influence of nitrogen nutrition, phosphorus nutrition, photon flux density, and ambient partial pressure of CO₂ during ontogeny. *Plant Physiol.* 78, 821–825.
- Wong, S.-C., Cowan, I.R., Farquhar, G.D., 1985b. Leaf conductance in relation to rate of CO₂ assimilation. 2. Effects of short-term exposure to different photon flux densities. *Plant Physiol.* 78, 826–829.
- Wong, S.-C., Cowan, I.R., Farquhar, G.D., 1985c. Leaf conductance in relation to rate of CO₂ assimilation. 1. Influences of water stress and photoinhibition. *Plant Physiol.* 78, 830–834.
- Woodward, F.I., Kelly, C.K., 1995. The influence of CO₂ concentration on stomatal density. *New Phytol.* 131, 311–327.
- Woodward, F.I., Williams, B.G., 1987. Climate and plant distribution at global and local scales. *Vegetatio* 69, 189–197.
- Zhu, G.H., Jensen, R.G., Bohnert, H.J., Wildner, G.F., Schlitter, J., 1998. Dependence of catalysis and CO₂/O₂ specificity of Rubisco on the carboxy-terminus of the large subunit at different temperatures. *Photosyn. Res.* 57, 71–79.